NASA TECHNICAL NOTE

NASA TN D-2554

C.1

NASA TN D-2554

MAGNETIC BREAKDOWN IN A FINITE ONE-DIMENSIONAL MODEL

by Gabriel Allen

Lewis Research Center

Cleveland, Ohio

NATIONAL AERONAUTICS AND SPACE ADMINISTRATION • WASHINGTON, D. C. • DECEMBER 1964

MAGNETIC BREAKDOWN IN A FINITE ONE-DIMENSIONAL MODEL

By Gabriel Allen

Lewis Research Center
Cleveland, Ohio

NATIONAL AERONAUTICS AND SPACE ADMINISTRATION

For sale by the Office of Technical Services, Department of Commerce,
Washington, D.C. 20230 -- Price $3.00

MAGNETIC BREAKDOWN IN A FINITE ONE-DIMENSIONAL MODEL

by Gabriel Allen

Lewis Research Center

SUMMARY

Exact solutions have been obtained of the Schroedinger equation for a model approximating an electron in a one-dimensional periodic potential acted on by a transverse uniform magnetic field. In this model the periodic potential is approximated by a finite chain (20 atoms long) of "periodic" square wells, and the parabolic potential due to the magnetic field is approximated by a parabolic square-well potential. Procedures are presented for obtaining solutions for arbitrary combinations of the well depth of the periodic potential V_0, the magnetic field strength H, and the ratio of well dimension (2w) to the atomic dimension (a), 2w/a. Eigenvalues and wave functions have been computed for the case $2w = a/2$ for several values of V_0 and H. The solutions obtained are valid for arbitrary field strengths, but in order to detect magnetic breakdown effects in such a short chain, very large values had to be used. Although the values of H in the computations were of the order of kilotesla (tens of megagauss), it has proved possible to associate these states with their zero-field counterparts. The subroutines used in the computations are also included.

INTRODUCTION

The study of the Fermi surface of metals became greatly accelerated following the publication of the often quoted papers in references 1 and 2. The profusion of theoretical and experimental papers on Fermi surfaces, which began soon afterwards, continues to the present day. Consequently, there is now available a veritable catalogue of quite detailed Fermi surfaces for a number of metals (ref. 3).

The results of parallel theoretical calculations were, for the most part, in such good agreement with the experimental results that various second-order features of the structure (e.g., spin-orbit splitting) could be examined in a meaningful way (refs. 4 to 6). One concept in which interest was revived is magnetic breakdown (refs. 6 to 10), a phenomenon in which the connectivity of a Fermi surface in a given direction may be changed in the presence of magnetic fields.

In all of the treatments of the effects of magnetic fields on the electrical properties of solids, computations can normally be carried out only for the extreme cases of very small or very large magnetic fields. It was felt that it might prove enlightening to examine an exact solution of even a simplified model that embodied some of the important features of the interaction in solids of electrons with external magnetic fields.

In this connection, in work done at the Lewis Research Center, exact solutions have been obtained for the case of an electron in a finite one-dimensional chain of "periodic" rectangular well potentials acted on by a uniform magnetic field in a direction perpendicular to that of the periodic potential. The periodic potential consisted of wells of width $2w$ separated by hills of width $2h = a - 2w$, where a, the distance between atomic centers, is the period. The solutions are valid for arbitrary values of a, w, and h.

Numerical values have been obtained for all of the bound-state eigenvalues and some of the eigenfunctions for $a = 3$ angstroms. Since the number of individual computations was a monotonic increasing function of the length of the chain, it was necessary to keep this length down to 20 atoms. The magnetic fields were then chosen to be large enough so as to make the effective magnetic potential comparable to the depth of the wells in the periodic potential. For a chain of this length (60 Å), the magnetic fields were, therefore, of the order of kilotesla (tens of megagauss).

It may be noted that the behavior of an electron subjected to such high fields in this model actually approximates that of electrons in real solids subjected to reasonable fields of the order of a few tesla. From a dynamical point of view, the field should be of such a size that the magnetic part of the potential becomes an appreciable fraction of the total potential over some part of the electron's path. In this model, the electron can travel a maximum distance of 60 angstroms before being scattered; therefore, fields of the order of kilotesla are required to build up the magnetic part of the potential in such a small distance. In real solids, on the other hand, the mean free path may be orders of magnitude greater than this, and much smaller magnetic fields could then accomplish the same objective.

It has been proved possible, however, to associate each of these states with its zero-field state. Thus, by following the wave function for the zero-field state to its high-field state, something may be learned about the behavior of the system for moderate or intermediate fields.

The computations were performed on the IBM 7094 at the Lewis Research Center, and the Fortran IV subroutines used are described and listed in the appendixes.

SYMBOLS

$\vec{A}$ vector potential

a distance between atomic centers, period

C_H constant defined by eq. (49)

c	velocity of light
E	parametrized quantity used like energy, see eq. (21)
E_F	Fermi energy
E_g	zero-field energy gap in band structure
e	charge of electron
G	$\lvert\gamma\rvert$
g	γ^2
H	magnetic field strength
$\vec{H}$	magnetic field
$H_n(\xi)$	n^{th} degree Hermite polynomial of argument ξ
H_z	magnitude of z component of magnetic field
h	half width of hill
$\hbar$	Dirac h, Planck's constant/2π
j	index specifying j^{th} atom from center
k_y, k_z	components of wave vector
m	mass of electron
m_x'	integer defined by eq. (19)
N	number of atoms in positive half of chain
n	integer defining the number of energy level, ϵ_n
$\vec{p}$	momentum
r	cyclotron radius
$S_n^w, \overline{S}_n^w$	determinants, see p. 38
$V(x)$	one-dimensional potential
$V_M(x')$	approximation to $V_{mag}(x')$, see eq. (17)
$V_{mag}(x')$	potential due to magnetic field, $1/2\ m\omega_c^2 x'^2$

$V_P(x), V_P(x')$	defined by eqs. (13) and (14), respectively
V_O	well depth of periodic potential
V_O'	energy due to magnetic field defined by eq. (18)
w	half width of well
x,y,z	coordinates
x'	$x - x_O$
x_O	defined by eq. (6)
γ	defined by eqs. (30) and (31)
ϵ	energy
ϵ_n	energy levels defined by eq. (9)
ν	integer defined by eq. (19b)
$\psi(\vec{r})$	wave function
ω_c	cyclotron frequency

Subscripts:

e	even solution
j	index specifying j^{th} atom from center
M	approximate magnetic
mag	magnetic
max	maximum
N	number of atomic distances from center of one end of chain counting central well as 0
P	periodic
SB	strong breakdown
WB	weak breakdown
x,y,z	coordinates
α,β	defined by eqs. (C15) to (C18)

Superscripts:

h hill

w well

$\bar{0}$, $\overset{-}{\underset{+}{0}}$ sign of appropriate g

DERIVATION OF WAVE EQUATION

Free Electrons in Magnetic Field

The wave equation describing a free electron in a constant magnetic field may be written as

$$\frac{1}{2m}\left(\vec{p} + \frac{e}{c}\vec{A}\right)^2 \psi(\vec{r}) = \epsilon\psi(\vec{r}) \tag{1}$$

where $\vec{A}$ is the vector potential, $\vec{p}$ is the momentum, and ϵ is the energy. The spin of the electron is neglected.

If the magnetic field $\vec{H}$ is given by $H_z\vec{k}$, where H_z is constant and $\vec{A}$ is chosen in the Landau gauge (ref. 11),

$$\vec{A} = H_z(0,x,0) \tag{2}$$

Then equation (1) may be written as

$$\frac{1}{2m}\left[p_x^2 + \left(p_y + \frac{e}{c}H_z x\right)^2 + p_z^2\right]\psi(x,y,z) = \epsilon\psi(x,y,z) \tag{3}$$

The substitution

$$\psi(x,y,z) = \lambda(x)\exp\left[i(yk_y + zk_z)\right] \tag{4}$$

will result in the following simplification of equation (3):

$$\frac{-\hbar^2}{2m}\frac{d^2\lambda}{dx^2} + \left[\frac{1}{2m}\left(\hbar k_y + \frac{e}{c}H_z x\right)^2 + \frac{1}{2m}\hbar^2 k_z^2\right]\lambda = \epsilon\lambda \tag{5}$$

Equation (5) is the equation of a harmonic oscillator centered about

$$x_0 = -\frac{c\hbar k_y}{eH_z} \tag{6}$$

with frequency

$$\omega_c = \frac{e}{mc}H_z \tag{7}$$

Thus, if $x' = x - x_0$, equation (5) may be written in the more familiar form

$$\frac{-\hbar^2}{2m}\frac{d^2\lambda}{dx'^2} + \frac{1}{2}m\omega_c^2 x'^2\lambda + \left(\frac{\hbar^2 k_z^2}{2m} - \epsilon\right)\lambda = 0 \tag{8}$$

From this form, it is known that

$$\epsilon_n - \frac{\hbar^2 k_z^2}{2m} = \omega_c\hbar\left(n + \frac{1}{2}\right)$$

or (using eq. (7))

$$\epsilon_n = \frac{\hbar^2 k_z^2}{2m} + \frac{eH_z}{mc}\hbar\left(n + \frac{1}{2}\right) \tag{9}$$

Thus, the allowed energy levels of a free electron in a constant magnetic field are given by equation (9).

The term $\lambda_n(x)$ will be a harmonic oscillator function in $(eH_z/c\hbar)(x - x_0)$. Thus,

$$\psi_{n,k_y,k_z} = \exp\left[i(yk_y + zk_z)\right]H_n\left[\sqrt{\frac{eH_z}{c\hbar}}(x - x_0)\right]\exp\left[\frac{-eH_z}{c\hbar}(x - x_0)^2\right] \tag{10}$$

where $H_n(\xi)$ signifies the n^{th} degree Hermite polynomial of the argument ξ. A further discussion may be found in reference 12.

Electron in One-Dimensional Periodic Potential and Constant Magnetic Field

If an electron is acted on simultaneously by a constant magnetic field $\vec{H} = H_z\vec{k}$ and a one-dimensional potential in the x-direction, then equation (1) must be replaced by

$$\left[\frac{1}{2m}\left(\vec{p} + \frac{e}{c}\vec{A}\right)^2 + V(x)\right]\psi(\vec{r}) = \epsilon\psi(\vec{r}) \tag{11}$$

When the previous substitutions are used in equation (11), it may be reduced to

$$\frac{-\hbar^2}{2m}\frac{d^2\lambda}{dx^2} + \left[\frac{1}{2m}\left(\hbar k_y + \frac{eH_z}{c}x\right)^2 + \frac{1}{2m}\hbar^2 k_z^2 + V(x)\right]\lambda = \epsilon\lambda \tag{12}$$

The following assumptions should now be made:

(1) The term $V(x)$ is a periodic potential $V_P(x)$ of period a such that

$$V_P(x) = 0 \qquad -w \le x \le w$$
$$= V_0 \qquad w \le x \le a - w \tag{13a}$$

and

$$V_P(x + na) = V_P(x) \tag{13b}$$

where n is any integer. Here w will be referred to as the well region.

(2) The term x_0 is a whole number of atomic distances. Assumption (2) will have the effect of making $V_P(x')$ periodic with the same period a as $V_P(x)$ since the center of a well region in x will coincide with the center of a well region in x' (equal to $x - x_0$) so that

$$V_P(x') = 0 \qquad -w \le x' \le w$$
$$= V_0 \qquad w \le x' \le a - w \tag{14a}$$

and

$$V_P(x' + na) = V_P(x') \tag{14b}$$

Then, the equivalent of equation (8) can be written as

$$\frac{-\hbar^2}{2m}\frac{d^2\lambda}{dx'^2} + \frac{1}{2} m\omega_c^2 x'^2\lambda + \left(\frac{\hbar^2 k_z^2}{2m} - \epsilon\right)\lambda + V_P(x')\lambda = 0 \tag{15}$$

The quantity $1/2\ m\omega_c^2 x'^2$, which will be called $V_{mag}(x')$, may be considered to be a potential due to the magnetic field. Then equation (15) can be written as

$$\frac{d^2\lambda}{dx'^2} + \frac{2m}{\hbar^2}\left\{\epsilon - \frac{\hbar^2 k_z^2}{2m} - \left[V_{mag}(x') + V_P(x')\right]\right\}\lambda = 0 \tag{16}$$

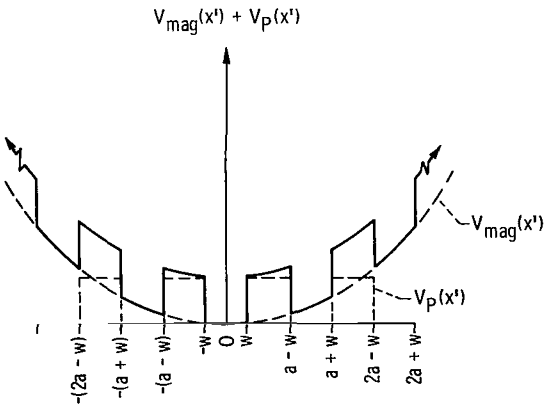

Figure 1. - Form of potential due to constant magnetic field and periodic square well. w = a/4.

The form of the potential $V_{mag}(x') + V_P(x')$ is shown in figure 1.

In each interval, the potential is like a harmonic oscillator in that it is parabolic in x'. The general solution to such a potential problem is a sum of two Weber functions (ref. 13), each of which has special behavior at the origin and at infinity. In an actual harmonic oscillator, only one of these functions serves as a wave function because of the requirement that wave functions be well behaved at infinity. Since each interval in the present problem is finite, however, neither of the Weber functions can be eliminated as an allowable solution, and the usual linear combination of two independent solutions of the second-order differential equation must be used for the wave function.

The form of the wave function is invariant throughout the entire range of x', the wave function for a given interval being distinguished entirely by the coefficients appropriate to that interval.

It may be noted that the symmetry which seems to be physically apparent in this problem in the form of the potential is somewhat obscured by the mathematical form of the wave function. The Weber functions for $-x$ are different from those for $+x$, and this fact must be taken into account when matching at $x' = 0$.

There is, in general, no actual physical symmetry here. The term $V_P(x')$ is symmetric about $x = 0$, whereas $V_{mag}(x')$ is symmetric about $x = x_0 = -c\hbar k_y/eH_z$. The special assumption has been made that x_0 is an integral number of atomic distances. As was already said, in such a case the entire potential $V_{mag}(x') + V_P(x')$ is symmetric in x'. Clearly this assumption will only be satisfied for special combinations of k_y and H_z.

However, the noncoincidence of the vertex of the parabola $V_{mag}(x')$ from the center of the well in $V_P(x')$ (see fig. 1) should not seriously affect the physical results as long as the resulting total potential does not differ greatly from the $V_{mag}(x') + V_P(x')$, which is the ordinate of figure 1. The depth of a well in the periodic part of the potential should be of the order of a few electron volts. The part of the potential due to the magnetic field turns out to be expressible as

$$V_{mag}(x') \approx 8.8\times10^{-10}\ H_z^2(x - x_0)^2\ \frac{\text{ev}}{(\text{Å})^2}$$

where H_z is in tesla, and $x - x_0$ is in angstroms.

The one-dimensional chain in the model is about 20 atoms long; therefore, magnetic fields large enough so that $V_{mag}(x')$ contributes a few electron volts before the chain ends should be used. Since there are 10 atoms on each side of the center, this means $V_{mag}(x') \approx 8\times10^{-9}\ H_z^2$ electron volt at the ends of the chain so that $H_z \approx 1$ kilotesla or 10 megagauss in order that $V_{mag}(x')$ contribute 1 electron volt to the total potential. Because the potential varies as $(x')^2$, $V_{mag}(x')$ will be much smaller than 1 electron volt over most of the chain so that a deviation from symmetry should have a relatively small effect on the results.

Approximation of Magnetic Potential by

Parabolic Square-Well Potential

Furthermore, a potential approximating $V_{mag}(x')$ should also not affect the results too drastically if it has the form

$$V_M(x') = m_{x'}^2 V_0' \tag{17a}$$

$$V_M(x' + na) = V_M(x') + (n^2 - \nu^2)V_0' \tag{17b}$$

where

$$V_0' = \frac{1}{2m}\left(\frac{eH_z}{c}\right)^2 a^2 \tag{18}$$

H is in tesla, n is any integer, and $m_{x'}$ is an integer depending on x' so that

$$m_{x'} = 0 \qquad 0 \leq x' \leq a - w \tag{19a}$$

$$m_{x'} = \nu \qquad \nu a - w \leq x' \leq (\nu + 1)a - w \qquad \nu \text{ any integer} \tag{19b}$$

The potential defined by equations (19) will be called a parabolic square-well potential.

Define

$$V(x') = \frac{2m}{\hbar^2}\left[V_M(x') + V_P(x')\right] \tag{20}$$

$$E = \frac{2m}{\hbar^2}\left(\epsilon - \frac{\hbar^2 k_z^2}{2m}\right) \tag{21}$$

where $V_M(x')$ is given by equations (17a) and (17b) and $V_P(x')$ is still given by equations (14).

The fact that the total potential is not periodic means that the wave function and its derivative must be matched at each boundary between regions of constant potential. This means that the rank of the determinant used for the determinantal compatibility condition is at least twice as large as the number of regions of constant potential in the positive half of the system (taking advantage of symmetry). Thus, in order to keep the determinant down to a manageable size, the system must be kept finite. This is readily accomplished by adding the cutoff condition

$$V[(N + 1)a - w] = \infty \tag{22}$$

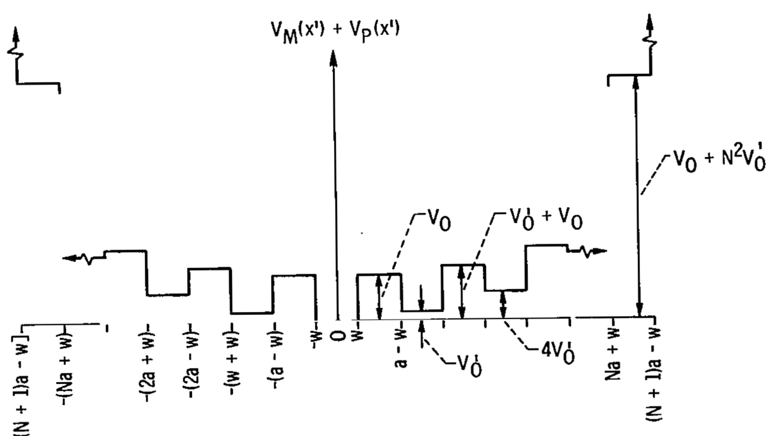

Figure 2. - Form of potential given by equations (20) and (22).

where N is the number of atoms in the positive half of the chain.

The form of $V(x')$ can be seen by examining $V_M(x') + V_P(x')$ which is shown in figure 2 (compare with fig. 1). The substitution of $V_M(x')$ for $V_{mag}(x')$ has the advantage that the solutions in each hill or well region are now combinations of trigonometric or hyperbolic functions rather than Weber functions. The effect of $V_M(x')$ is a kind of averaging of $V_{mag}(x')$ in any region considered. The averaging could be improved by using $(m_{x'}^2 + m_{x'} + 1/3)V_0'$ instead of $m_{x'}^2 V_0'$. When considering the nature of the approximations already inherent in the model, however, the indicated improvement would be second order at best.

Another factor that must be considered is the effect of the cutoff as given by the boundary condition in equation (22). It is clear from figures 1 and 2 that the effect of the cutoff will be small for states lying well below $V_0 + N^2V_0'$, since the wave functions would have small amplitudes when $x' < (N + 1)^2a - w$ even if there were no cutoff. The energies for a few of the states investigated were not really low enough to avoid a forcing of the wave function to zero in the vicinity of $x' = (N + 1)^2a - w$. Most of the states examined are not greatly affected by the condition in equation (22), however.

SOLUTION OF WAVE EQUATION

Derivation of Wave Function

When the quantities defined by equations (20) and (21) are used, the wave equation for $\lambda(x')$ becomes

$$\frac{d^2\lambda}{dx'^2} + [E - V(x')]\lambda = 0 \tag{23}$$

The solution of equation (23) is readily obtained. Denote the region from $-a$ to a as the 0^{th} region. This is the region for which $V_M(x') = 0$. Furthermore, denote the interval by a subscript (starting with 0) and indicate by an h or w superscript whether the periodic part of the potential is "on" (hill) or "off" (well). Then in the 0^{th} well,

$$\lambda_0^w(x') = C_0^w \sin \gamma_0^w x' + D_0^w \cos \gamma_0^w x' \qquad -w \leq x' \leq w \tag{24}$$

and in the 0^{th} hill,

$$\lambda_0^h(x') = C_0^h \sin \gamma_0^h x' + D_0^h \cos \gamma_0^h x' \qquad w \leq x' \leq a - w \tag{25}$$

where the C's and D's are constants and

$$\gamma_0^w = \sqrt{E} = \sqrt{\frac{2m}{\hbar^2}}\left(\epsilon - \frac{\hbar^2 k_z^2}{2m}\right)^{1/2} \tag{26}$$

$$\gamma_0^h = \sqrt{\frac{2m}{\hbar^2}}\left(\epsilon - \frac{\hbar^2 k_z^2}{2m} - V_0\right)^{1/2} \tag{27}$$

An analogous expression exists for the wave function in the 0^{th} hill for negative x'; that is, $-(a - w) \leq x' \leq - w$.

In the n^{th} interval,

$$\lambda_n^w(x') = C_n^w \sin \gamma_n^w x' + D_n^w \cos \gamma_n^w x' \qquad na - w \leq x' \leq na + w \tag{28}$$

$$\lambda_n^h(x') = C_n^h \sin \gamma_n^h x' + D_n^h \cos \gamma_n^h x' \qquad na + w \leq x' \leq (n + 1)a - w \tag{29}$$

where

$$\gamma_n^w = \sqrt{\frac{2m}{\hbar^2}}\left(\epsilon - \frac{\hbar^2 k^2}{2m} - n^2 V_0'\right)^{1/2} \tag{30}$$

and

$$\gamma_n^h = \sqrt{\frac{2m}{\hbar^2}}\left(\epsilon - \frac{\hbar^2 k_z^2}{2m} - n^2 V_0' - V_0\right)^{1/2} \tag{31}$$

Equations (28) and (29) are of the proper form only for real positive γ_n's. The other possibilities will be shown subsequently.

Both even and odd solutions exist, in general. The even solutions will be discussed in detail and necessary modifications in procedure for odd solutions will be indicated where relevant.

The form of the solution in the 0^{th} well becomes (subscript e denotes an even solution)

$$\lambda_{0,e}^w(x') = D_{0,e}^w \cos \gamma_{0,e}^w x' \qquad -w \leq x' \leq w \tag{32}$$

The solutions in the other intervals maintain the same forms as given by equations (30) and (31), but pains must be taken to use the even coefficients and eigenvalues. Thus,

$$\lambda_{n,e}^w(x') = C_{n,e}^w \sin \gamma_{n,e}^w x' + D_{n,e}^w \cos \gamma_{n,e}^w x' \qquad na - w \leq x' \leq na + w \tag{33}$$

and

$$\lambda^{h}_{n,e}(x') = C^{h}_{n,e} \sin \gamma^{h}_{n,e}x' + D^{h}_{n,e} \cos \gamma^{h}_{n,e}x'$$

$$na + w \leq x' \leq (n + 1)a - w \qquad (34)$$

where

$$\gamma^{w}_{n,e} = \sqrt{E_{n,e}} \qquad (35a)$$

$$\gamma^{h}_{n,e} = \sqrt{E_{n,e} - \frac{2m}{\hbar^2} V_0} \qquad (35b)$$

and

$$E_{n,e} = E_e - n^2 \frac{2m}{\hbar^2} V_0' \qquad (36)$$

The term E_e is an eigenvalue of equation (23) belonging to an even eigenfunction.

It will be convenient to write the wave function in each interval in such a form that it is centered about one of the boundaries of the given interval. Dropping the e subscript for simplicity results in

$$\lambda^{w}_{0}(x') = B^{w}_{0} \cos \gamma^{w}_{0}x' \qquad -w \leq x' \leq w \qquad (37)$$

$$\lambda^{w}_{n}(x') = A^{w}_{n} \sin \gamma^{w}_{n}\Big[x' - (na - w)\Big] + B^{w}_{n} \cos \gamma^{w}_{n}\Big[x' - (na - w)\Big]$$

$$na - w \leq x' \leq na + w \qquad (38)$$

$$\lambda^{h}_{n}(x') = A^{h}_{n} \sin \gamma^{h}_{n}\Big[x' - (na + w)\Big] + B^{h}_{n} \cos \gamma^{h}_{n}\Big[x' - (na + w)\Big]$$

$$na + w \leq x' \leq (n + 1)a - w \qquad (39)$$

and

$$\lambda^{h}_{N}(x') = A^{h}_{N} \sin \gamma^{h}_{N}\Big\{x' - \Big[(N + 1)a - w\Big]\Big\} \qquad (40)$$

where the coefficients are all linear combinations of the C's and D's in equations (33) and (34), $B^{w}_{0} \equiv D^{w}_{0,e}$, the γ's are given by equations (35), and N is the number of atomic distances from the center to one end of the chain counting the central well as 0. It should be noted that λ^{w}_{0} is centered about $x' = 0$; the arguments of λ^{w}_{n} and λ^{h}_{n} are zero at the left boundary of the appropriate interval, and the argument of λ_N is zero at the boundary at which the potential becomes infinite and the wave function vanishes (which is the right boundary of the last interval).

As has been stated previously, solutions of the form shown are for real nonzero γ's. If, for some eigenvalue ϵ, γ in some interval (say the j^{th}) is zero, then in that interval

$$\lambda_j(x') = A_j\Big[x' - (ja \pm w)\Big] + B_j \tag{41}$$

where the + or - occurs according to whether the interval in question is a hill or well region, respectively.

Finally, if γ is imaginary in some interval, the trigonometric functions become the corresponding hyperbolic ones and the general form remains unchanged. Quantities g and G are defined as follows:

$$g = \gamma^2 \tag{42}$$

$$G = |\gamma| \tag{43}$$

The form of the solution in a given interval will then be determined by the sign of g in the interval. (Note that g_0^W is always greater than 0.) Use will be made of the well-known properties $\sin i\alpha = i \sinh \alpha$ and $\sinh i\alpha = i \sin \alpha$ in the expressions that are used for $\lambda(x')$. Also, at this point the coefficients A will be redefined in such a way that the transition between positive and negative g values will be smooth. A summary of the different forms of $\lambda(x')$ in various regions is

$$\lambda_0^W(x') = B_0^W \cos G_0^W x' \tag{44}$$

where $-w \leq x' \leq w$,

$$\lambda_n^W(x') = \begin{cases} \dfrac{A_n^W}{G_n^W} \sinh\Big[G_n^W\, x' - (na - w)\Big] + B_n^W \cosh G_n^W\Big[x' - (na - w)\Big] & g_n^W < 0 \\[2ex] A_n^W\Big[x' - (na - w)\Big] + B_n^W & g_n^W = 0 \\[2ex] \dfrac{A_n^W}{G_n^W} \sin G_n^W\Big[x' - (na - w)\Big] + B_n^W \cos G_n^W\Big[x' - (na - w)\Big] & g_n^W > 0 \end{cases} \tag{45}$$

where $na - w \leq x' \leq na + w$,

$$
\lambda_n^h(x') = \begin{cases} \dfrac{A_n^h}{G_n^h} \sinh G_n^h\left[x' - (na + w)\right] + B_n^h \cosh G_n^h\left[x' - (na + w)\right] & g_n^h < 0 \\ A_n^h\left[x' - (na + w)\right] + B_n^h & g_n^h = 0 \\ \dfrac{A_n^h}{G_n^h} \sin G_n^h\left[x' - (na + w)\right] + B_n^h \cos G_n^h\left[x' - (na + w)\right] & g_n^h > 0 \end{cases} \tag{46}
$$

where $na + w \leq x' \leq (n + 1)a - w$, and

$$
\lambda_N^h(x') = \begin{cases} \dfrac{A_N^h}{G_N^h} \sinh G_N^h\left\{x' - \left[(N + 1)a - w\right]\right\} & g_N^h < 0 \\ A_N^h\left\{x' - \left[(N + 1)a - w\right]\right\} & g_N^h = 0 \\ \dfrac{A_N^h}{G_N^h} \sin G_N^h\left\{x' - \left[(N + 1)a - w\right]\right\} & g_N^h > 0 \end{cases} \tag{47}
$$

where $Na + w \leq x' \leq (N + 1)a - w$.

Eigenvalues. - The determinantal compatibility condition from which the eigenvalues may be determined can be obtained by matching the wave function and its first derivative at each of the boundaries. The details are given in appendix A. The determinant is large and unwieldy, but fortunately a systematic procedure for evaluating it in general could be formulated. A subroutine was devised from which the results could be obtained on the IBM 7094. Figures 3(a) to (e) show the eigenvalues for a chain of 10 atoms on each side of the 0^{th} well plotted as a function of magnetic field strength (by using V_0'). Each figure represents a fixed periodic well depth (V_0). Note that the eigenvalues are actually $\epsilon - \hbar^2 k_z^2/2m$ rather than ϵ (see eqs. (30) and (31)).

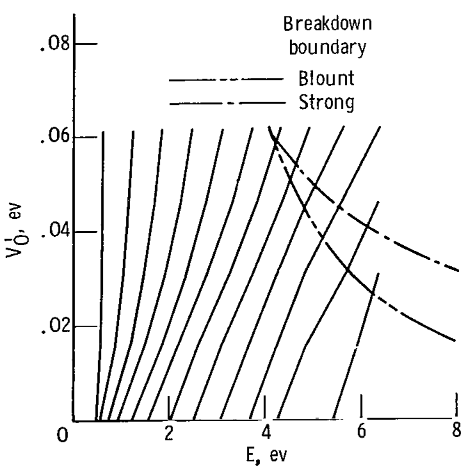

(a) Even eigenvalues; V_0, 1 electron volt.

Figure 3. - Eigenvalues as function of V_0'.

Wave functions. - The matching conditions that are used collectively to obtain the eigenvalues can now be used individually in succession to find the ratios of the coefficients in each interval to some given coefficient that will remain arbitrary except for normalization. The coefficient of the 0^{th} well B_0^w has been

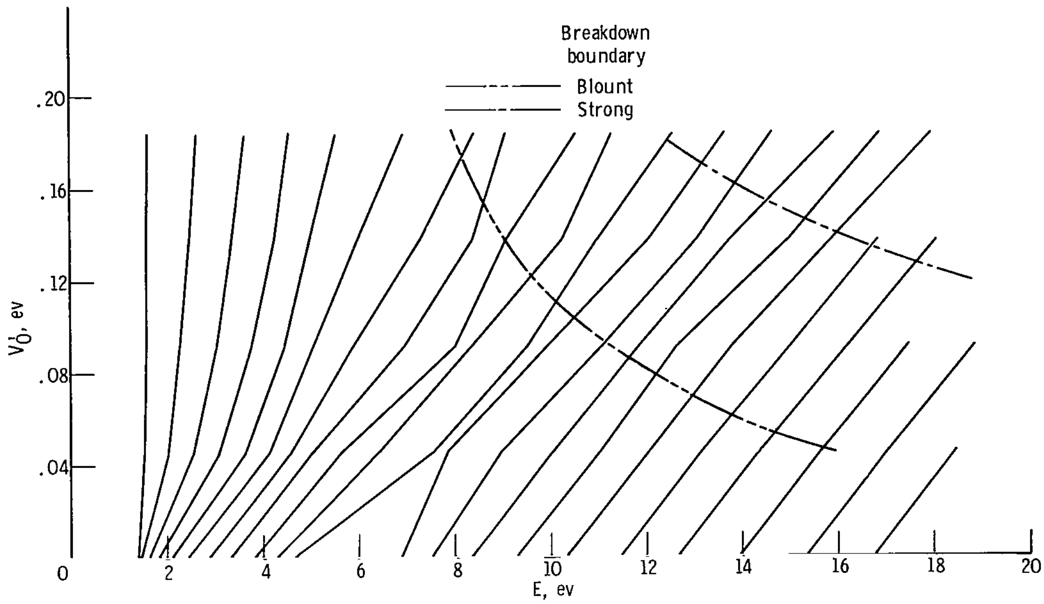

(b) Even eigenvalues; V_0, 3 electron volts.

Figure 3. - Continued. Eigenvalues as function of V_0'.

chosen as the arbitrary coefficient, and all of the other coefficients have been obtained in terms of it. The details are shown in appendix B.

In order to compare the behavior of different states, it is convenient to use normalized wave functions. The normalization is shown in appendix C.

MAGNETIC BREAKDOWN IN MODEL

In order to see what magnetic breakdown means as applied to this model, the behavior of the system may be examined as the magnetic field increases, and an attempt to account for the changes in a reasonable way may be made. There are a few guidelines that may be laid out in advance without (it is hoped) prejudicing the interpretation.

When there is no magnetic field, the system may be described as an electron interacting with a periodic square-well potential in a box. There is a basic objection to the use of ordinary perturbation theory in estimating the effect of magnetic fields on the properties of laboratory sized samples (ref. 14). In fact, it is the periodic part of the potential that is commonly treated as a perturbation to describe the behavior of systems under the influence of both a periodic potential and magnetic fields (refs. 7 to 10). Nevertheless, the behavior of the system will change in a continuous manner as the magnetic field enters the picture. Speaking qualitatively, very small fields should have a relatively insignificant effect, and, as the fields increase, their effect should become more easily perceptible. Therefore, some measure may be sought that might be expected to indicate when the size of the field is such as to have readily discernible effects on the behavior of the system.

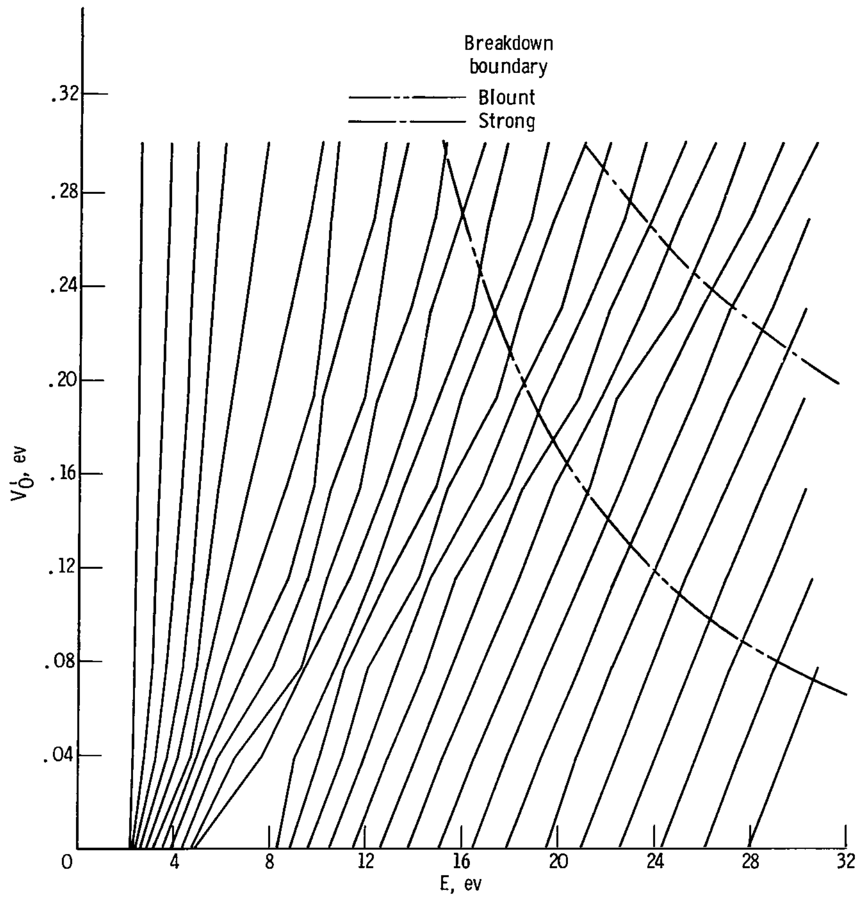

(c) Even eigenvalues; V_0, 5 electron volts.

Figure 3. - Continued. Eigenvalues as function of V_0'.

Perhaps the simplest and most naive measure that comes to mind is a comparison of the magnitude of the magnetic potential with V_0, the depth of the well in the periodic potential. When equations (17) are used, this condition may be written as

$$V_M(x') = V_0 \tag{48}$$

The conditions described by equation (48), in which somewhere in the chain $V_M(x')$ becomes as large as V_0, will be referred to as weak breakdown (WB). More explicitly, define

$$C_H = \frac{1}{2m}\left(\frac{e}{c}\right)^2 = 8.793984\times10^{-10} \frac{\text{ev}}{(\text{Å})^2(\text{tesla})^2} \tag{49}$$

and define n_{WB} to be the value of ν in equation (19) at weak breakdown. Then V_0' is expressible as

$$V_0' = C_H a^2 H^2 = \frac{1}{2} m\omega_c^2 a^2 \tag{50}$$

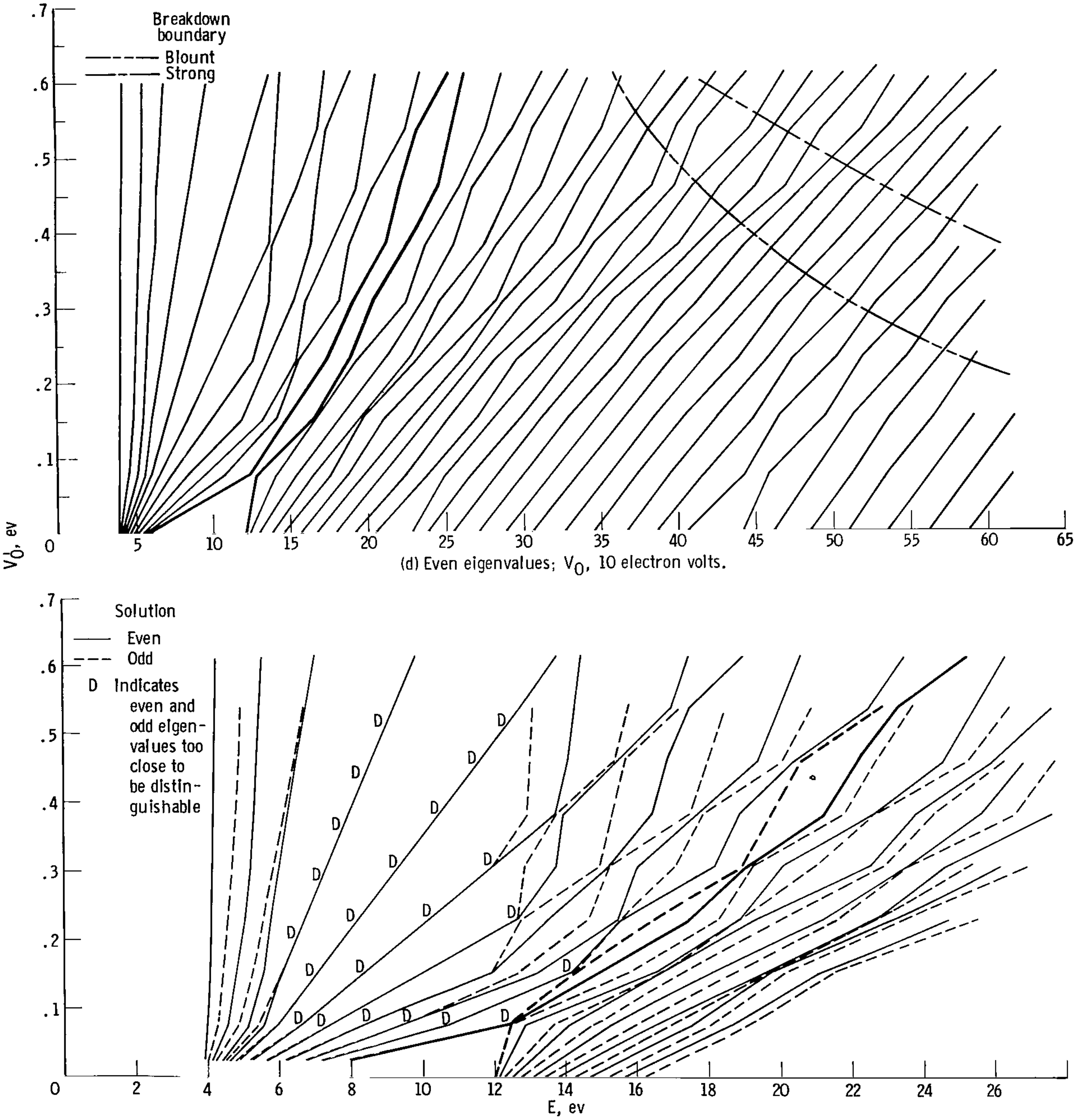

(e) Blowup of lower energy portion; V_0, 10 electron volts.

Figure 3. - Concluded. Eigenvalues as function of V_0'.

and V_M at weak breakdown is

$$(V_M)_{WB} = C_H H^2 n_{WB}^2 a^2 = V_0 \tag{51}$$

Furthermore,

$$n_{WB} = \sqrt{\frac{V_0}{C_H H^2 a^2}} \tag{52}$$

$$H_{WB} = \sqrt{\frac{V_0}{C_H (n_{WB} a)^2}} \tag{53}$$

There is a second type of breakdown that may be called strong breakdown. In this situation, the change in V_M over a distance a equals V_0, so that the magnetic potential "washes out" the periodic potential. Thus,

$$a \frac{\Delta V_M(x')}{\Delta x'} = V_0 \tag{54}$$

so that letting the subscript SB denote strong breakdown enables V_M to be expressed as

$$(V_M)_{SB} = C_H H^2 (n_{SB} a)^2 \tag{55}$$

$$n_{SB} = \frac{V_0}{2C_H H^2 a^2} \tag{56}$$

and

$$H_{SB} = \sqrt{\frac{V_0}{2C_H n_{SB} a^2}} \tag{57}$$

Recently, a quite different criterion for breakdown has proved useful in explaining certain experimental results (refs. 7 to 10). This condition is sometimes called Blount breakdown and for an infinite crystal is commonly expressed in the form

$$\frac{E_g^2}{\hbar\omega_c E_F} \approx 1 \tag{58}$$

where E_g is the zero-field energy gap in the band structure and E_F is the Fermi energy.

In this model, if it is assumed that an eigenvalue E plays the role of E_F, Blount's criterion becomes

$$H \approx 8 \times 10^3 \frac{E_g^2}{E} \text{ tesla} \tag{59}$$

or in terms of V_0',

$$V_0' \approx \frac{0.5 \times E_g^4}{E^2} \text{ ev} \tag{60}$$

It may be seen from figure 3 that actual gaps at zero field can be found, and these gaps may be used directly for E_g instead of resorting to first-order perturbation theory as is more commonly done (ref. 10).

RESULTS AND DISCUSSION

Description of Specific Model

First, numerical values for the specific model used in the computations will be given. A value of 3 angstroms for a has been chosen as representative of a large number of actual solids. It should be emphasized that the results in the preceding section are valid for all values of a, w, h, and H_z. In this report, the computations have, nevertheless, been limited to the case

$$2w = 2h = a/2 = 1.50 \text{ Å} \tag{61}$$

With this value of a, equation (18) is expressible as

$$V_0' = 7.9 \times 10^{-9} H_z^2 \frac{\text{ev}}{(\text{tesla})^2}$$

Next the length of the chain was fixed by the time required for the subroutines to go through a set of eigenvalues for fixed V_0 and V_0'. It turned out that a chain 10 atoms on each side of the 0^{th} well had a determinant of such a size that a set (with fixed V_0 and V_0') could run in the maximum allowed time of 5 minutes. Thus, N was set equal to 10 in the computations.

Eigenvalues

The actual Fortran IV subroutines used in the computations are described in appendix D. The eigenvalues for various well depths are shown as a function of magnetic field strength (or V_0') in figure 3. For each V_0, computations have been carried out for a few values of V_0' and these points connected by straight lines. (This procedure accounts for the kinks in the figures.) Figures 3(a) to 3(d), however, show only even eigenvalues, while eigenvalues obtained from odd and from even solutions are shown in figure 3(e). These eigenvalues are distinguished on the figures (where possible) by broken and solid lines, respectively. It may be noted that the chain in the model was long enough for the system to show a clear-cut band structure at zero field. As can be seen, the magnetic field shifts these zero-field levels by unequal amounts. Thus, the energy gaps in the band structure E_g (which are zero-field concepts in ordinary band-structure language) would be difficult to discern at large fields were it not for the fact that they were connected to the zero-field positions.

Some of the even and odd levels for higher fields are almost degenerate. These situations are denoted by a D at the energy in question. The actual computations that were performed using double-precision arithmetic show that in every case there was a nonzero separation between even and odd evergy levels. The pattern was always such that for a given V_0 and V_0' the lowest state is even, and then alternate odd and even states follow as far out as the computations were carried. This is certainly to be expected and was only used as a rough check to see if any states were skipped in the eigenvalue search routine.

Certain features to be expected if an actual band structure were observed were common to the eigenvalues of the system independent of the well depth and are shown for $V_0 = 10$ in figure 3(e). First of all, there were always 21 eigenstates in the first band. The lowest eigenstate was always even, and the eigenstate at the top of the first band was also even. The lowest state in the second band was therefore odd.

Since it was intended to examine the three types of breakdown described in the preceding section, it was necessary to examine states in potentials for which strong breakdown had occurred. As a margin of safety for each value of V_0, computations were made up to eigenvalues 50-percent larger than the value of the pertinent $(V_M)_{SB}$.

In this connection, it may be mentioned that, in order for the effects of strong breakdown to be manifest, the energy of the state being examined should be high enough so that the wave function has an appreciable amplitude in the region where the slope of $V_M(x')$ is changing rapidly enough to wash out the effect of $V_P(x')$ (see eq. (54)). Thus, strong breakdown will be said to occur in this model whenever the system is in an eigenstate such that $E \gtrsim (V_M)_{SB}$. When equations (50) and (55) are used, the equation of the strong breakdown boundary is

$$E = \frac{V_0^2}{4V_0'} \tag{62}$$

Both strong and Blount breakdown lines are indicated in the figures. The Blount boundary was plotted by using the actual gaps taken from the figures for E_g in equation (60).

Figure 4 shows the shifting of the eigenvalues by increasing the well depth at a constant magnetic field. It may be noted that, for small well depths, the separation between successive eigenvalues does tend, as V_0 goes to zero, to approach the constant value $\hbar\omega_c$ (equal to 0.322 ev for the field chosen) as given by equations (7) and (9). It should be mentioned that the states on the E-axis which represent zero well depth are the actual values for a free electron in a magnetic field computed from equation (9). If the eigenvalues for $V_0 = 0$ in figure 2 are computed, the lower states ($E \leqq 7$ ev) are rather close to those on the E-axis in figure 4, but the separation for the higher states becomes rather large (approximately 0.7 ev between the last two eigenvalues shown).

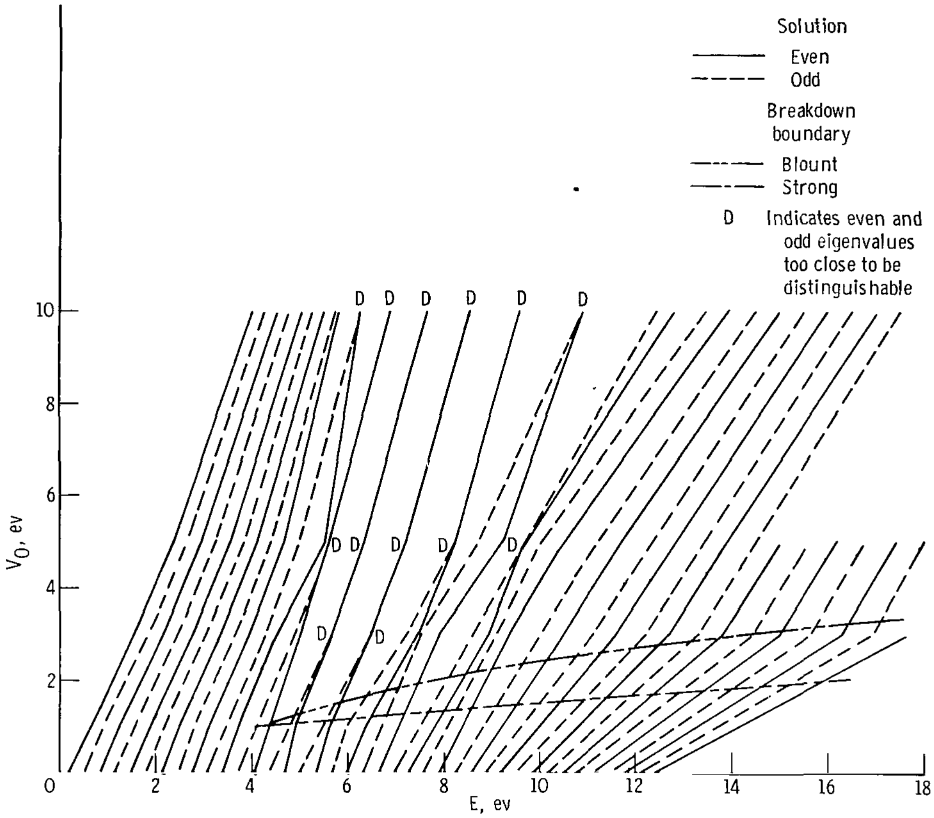

Figure 4. - Effect of well-depth at constant magnetic field of 2.8 kilotesla (28 megagauss). Values at $V_0 = 0$ are eigenvalues for free electron in magnetic field obtained from equation (10).

For the lower eigenstates, there seems to be a slight decrease in separation as V_0 increases. For the higher lying states in the first band, however, the eigenvalues seem to cluster in degenerate odd-even pairs separated by about 1 electron volt. A comparison with figure 3 shows that the degeneracy is lifted after crossing the gap between the first and second bands.

As the well depth increases, it is tempting to search for any tendency for the states to spread into a band (line broadening) as described in reference ence 10. However, this broadening arose from the degeneracy in the position of x_0 of each state at fixed V_0'. By contrast, the computations in the present model were made at a fixed x_0, so that there is no reason for the effect to show up in the model.

Wave Functions

The actual subroutines used in these computations are described in appendix E. In order to learn more about individual states, it is helpful to look at the wave functions. Wave functions have been computed and plotted for a large number of eigenvalues and some of the characteristics that were found are shown here. Advantage has been taken of symmetry so that the plots show only the positive half of the chain.

Most of the wave functions shown are for a rather deep well ($V_0 = 10$ ev). Some wave functions for shallower wells have been computed and do not seem to differ qualitatively from these. Therefore, the discussion will be limited to this well depth unless the contrary is specified.

The preceding discussion of the eigenvalues shown in figure 3 contended that the lines connecting the eigenstates could be interpreted as showing the change in the zero-field states as V_0' increased. At a given V_0', the wave function for the lowest eigenvalue found (which is always even) has no nodes over the entire 20-atom chain; the wave function for the next one (which is odd) has one node at $x' = 0$, and the wave function for each successive eigenvalue has one more node than its predecessor. The wave function corresponding to the i^{th} eigenvalue thus has $i - 1$ nodes for any V_0'. This fact makes it possible to follow the change in behavior of the i^{th} state of the system in configuration space as V_0' varies and permits a connection to be made between high-field and zero-field states. Of course, this test is not a sufficient one, since zero-field states could cross one another as the magnetic field increases. Thus, some additional factors will be considered in examining the behavior of the wave function to support the identification with indicated zero-field states in figures 3 and 4.

In the discussion which follows, it should be noted that the number of nodes in the wave function for the 20-atom chain for even and odd solutions is, respectively, twice the number to the right of $x' = 0$ and twice the number plus 1.

Another point requires some clarification. For a given eigenstate, A_N^h is determined by matching the wave function at the boundary between the last well and the last hill (where $x' = 10a + w$). Naturally, the vanishing of the determinant in appendix A is just the condition required to ensure that A_N^h would be exactly the same for this eigenstate if it had been computed by matching the $d\lambda(x')/dx'$ rather than $\lambda(x')$ itself at this boundary. If the determinant for a given eigenstate is sufficiently close to zero, then $d\lambda(x')/dx'$ is smooth everywhere. If it is not sufficiently close to zero, $\lambda(x')$ is smooth but $d\lambda(x')/dx'$ is discontinuous at $x' = 10a + w$ and the amplitude of $\lambda(x')$ is inordinately large in this region.

It turned out that it was not possible to match the boundary conditions with needed accuracy for all the eigenvalues. For this reason, a somewhat incomplete set of wave functions is presented, in the sense that the same state can not always be followed for different magnetic fields. The figures show wave functions for states satisfying conditions as closely as were available under the circumstances.

In this connection, it should be mentioned that the odd wave functions were most frequently inaccurate, and therefore, all of the figures show only even states except where otherwise indicated. As mentioned in the preceding section, the bottom of the second band is always an odd state. It is necessary to keep in mind that the lowest even state in the second band that is shown in several of the figures is actually the second state in the second band.

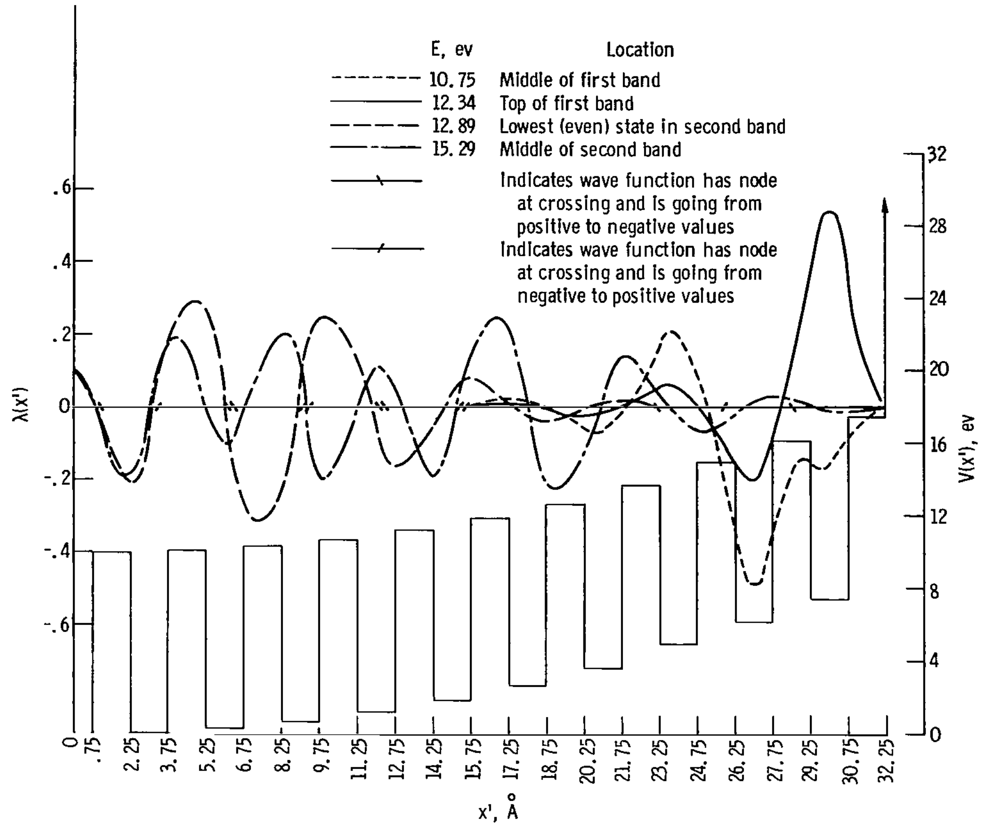

Figure 5. - Wave functions for eigenstates at a magnetic field strength of 3.1 kilotesla; V_0', 0.0765 electron volt.

The general features of the wave functions for the system will be examined in some detail. Figure 5 is typical and represents the system in a field of 3.1 kilotesla (31 megagauss, $V_0' = 0.0765$ ev). The lowest state in the figure is for $E = 10.75$ electron volts. This state is in the first band and has 18 nodes. The amplitude of this state has a definite maximum at about 27 angstroms and is very small for $x' < 22$ angstroms.

The next state shown is at the top of the first band ($E = 12.34$ ev). The general appearance of this wave function is quite similar to that of the preceding state shown except that the maximum is even more pronounced and is shifted slightly to $x' = 30$ angstroms.

The state following this one, although rather close to it in energy ($E = 12.89$ ev), demonstrates a sharply different character. For this state the amplitude is suddenly quite large in the vicinity of $x' = 0$ (although the maximums are not as pronounced as for the two preceding states) and is very small for $x' \gtrsim 17$ angstroms.

The last state shown in figure 5 is for $E = 15.29$ electron volts and is in the middle of the second band. It shares with the preceding state a low amplitude near the end of the chain and a comparatively large one near the center.

Some semiquantitative statements may be made about this behavior instead of a full quantitative explanation. First of all, an explanation may be sought from the viewpoint that, in the first band, the system is largely controlled by the magnetic field with even the relatively deep (10 ev) "periodic" well having no more than a modulating effect on the basic free electron in a magnetic field behavior. In this framework, it is proper to consider the cyclotron radius $\hbar k/m\omega_c$ as the primary parameter governing the motion of the electron. For a field of 3.1 kilotesla (31 megagauss), this quantity is

$$r \approx 6.35 \sqrt{n + 1/2} \text{ Å} \tag{63}$$

where n is the number of the state in equation (9).

The state $E = 10.75$ electron volts is the 19th state, and so r should be about 27.3 angstroms, which is quite close to the peak of 27 angstroms for this state. The state at the top of the first band is the 23rd state, and, for it, r will be about 30.8 angstroms, which is still not far from the sharp peak at 30 angstroms.

The next state, being at (or near) the bottom of the second band, may be expected to behave quite differently since it is on the other side of what would be the Brillouin zone for a truly periodic potential (see fig. 3(e)). It might be expected to behave more like a state near the bottom of the first band, so since it is the second state (the lowest state in the second band is odd), n may be set equal to 2 in obtaining an estimate of r. The resulting value of about 10 angstroms is not far from the actual region of large amplitude for this state. The final state in the middle of the second band behaves like a state that is less bound by the magnetic field than the others, and considering the fact that its energy is comparatively high, this is not surprising.

Another way of looking at the problem is to consider the motion in the k_x - k_y plane. States well below the top of the first band have orbits in k-space that do not come too close to the Brillouin zone. The state at the top of the first band has an orbit in k-space much of which is near the Brillouin zone boundary. On the other hand, the states near the bottom of the second zone have orbits in the second Brillouin zone and, in the reduced zone scheme, these are again not very close to the zone boundary.

The same general type of behavior is shown in figure 6 for states at $H = 6.2$ kilotesla (62 megagauss). It is noted that $r = 21.8$ angstroms for $n = 23$ at this field and again this is very close to the position of the sharp maximum for the top of the band. The simple picture fails for the state in the middle of the band though, since no very clear maximum is present, and secondly, r would be about 19 angstroms, which is a rather low amplitude point here. Nevertheless, the overall behavior is quite similar to that shown in figure 5.

Some additional weight to this interpretation is furnished by figures 7 to 9. Figures 7 and 8 show some odd wave functions that adequately satisfy the matching requirements. Figure 7 shows the states at $H = 3.1$ kilotesla

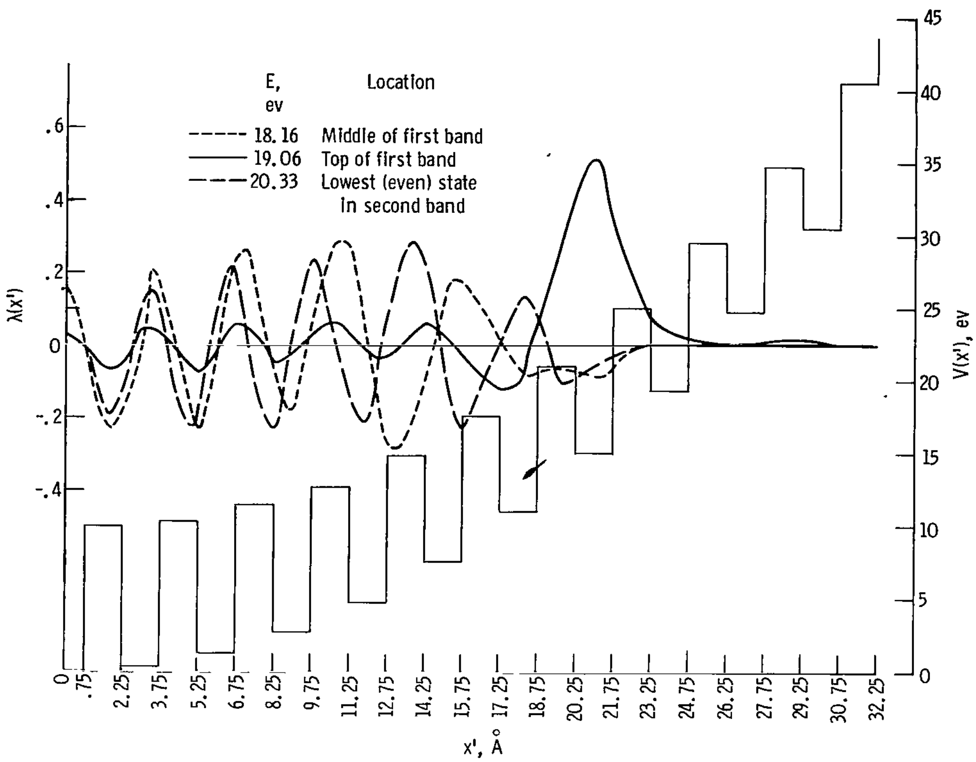

Figure 6. - Wave functions for eigenstates at a magnetic field strength of 6.2 kilotesla; V_0', 0.3061 electron volt.

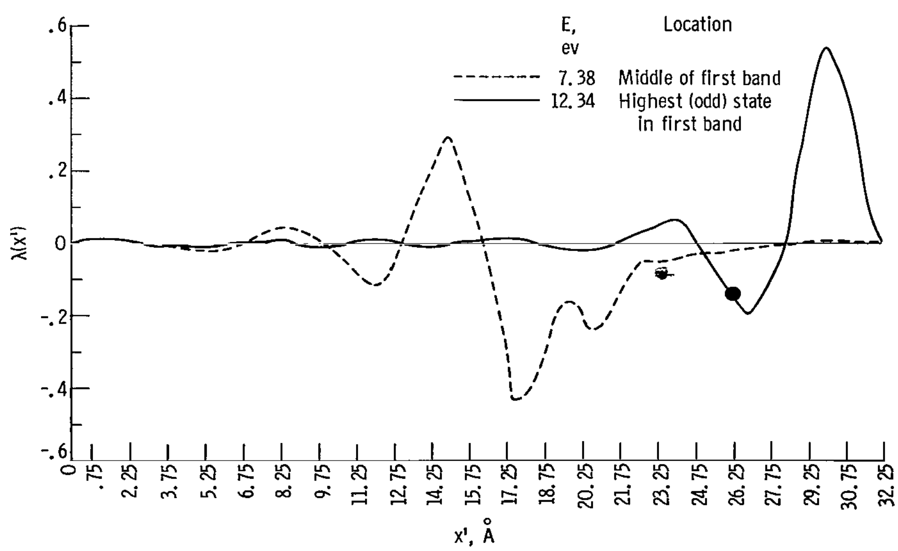

Figure 7. - Odd wave functions in first band; magnetic field strength, 3.1 kilotesla.

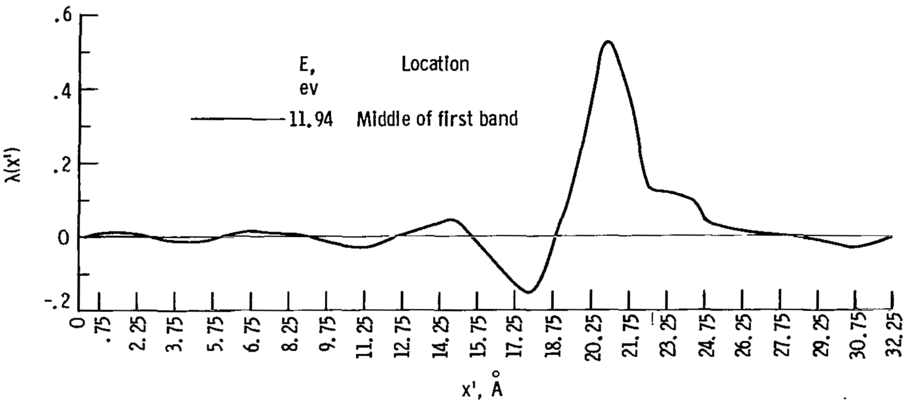

Figure 8. - Odd wave function in first band; magnetic field strength, 4.4 kilotesla.

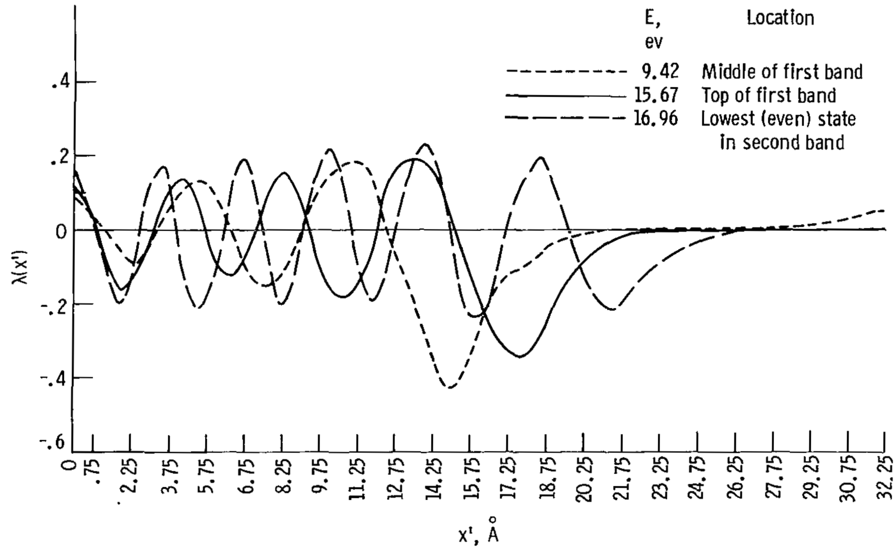

Figure 9. - Even wave functions for well depth of 5 electron volts; magnetic field strength, 5.9 kilotesla.

(31 megagauss, compare with fig. 5). The wave functions would fit in properly with those shown in figure 5, and r would be 24 angstroms for the state in the middle of the band (not very good agreement) and 30 angstroms for the state near the top of the band (quite good agreement).

Figure 8 shows an odd wave function in the middle of the first band for a field of 4.4 kilotesla (44 megagauss). The peak is at 21 angstroms, which is in very good agreement with r for this field strength.

Some wave functions for a smaller well depth (V_0 = 5 ev) are shown in figure 9. Again the same general features as in figures 5 and 6 are exhibited.

Thus, it would appear that the general behavior of the system described for figure 5 occurs under a variety of conditions. The picture used as a description is too simple to be expected to apply uniformly to a more complete examination of wave functions for all combinations of well depth and magnetic field strength. Nevertheless, it appears to be somewhat useful in a limited

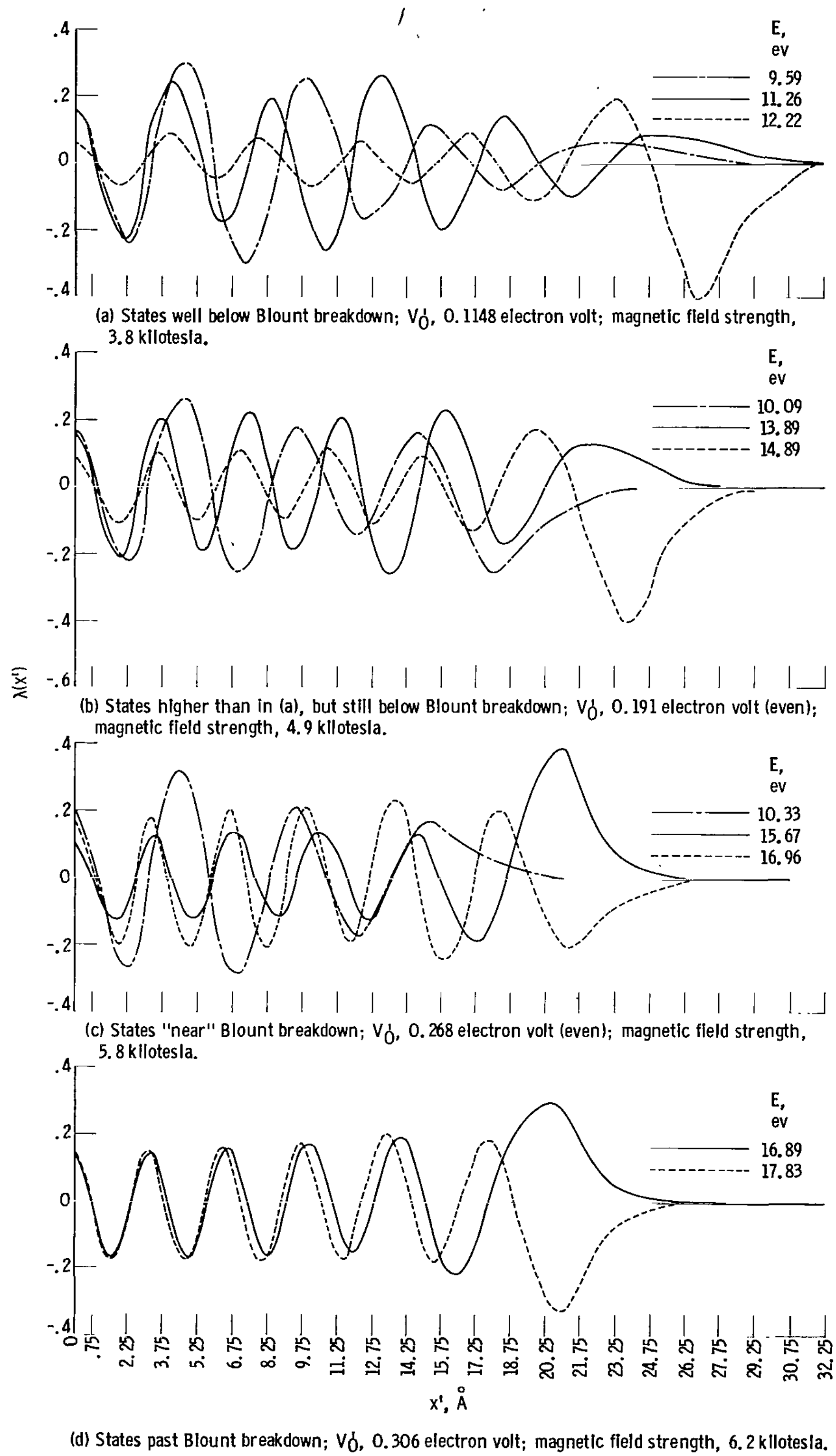

(a) States well below Blount breakdown; V_0', 0.1148 electron volt; magnetic field strength, 3.8 kilotesla.

(b) States higher than in (a), but still below Blount breakdown; V_0', 0.191 electron volt (even); magnetic field strength, 4.9 kilotesla.

(c) States "near" Blount breakdown; V_0', 0.268 electron volt (even); magnetic field strength, 5.8 kilotesla.

(d) States past Blount breakdown; V_0', 0.306 electron volt; magnetic field strength, 6.2 kilotesla.

Figure 10. - Blount breakdown in model; V_0, 5 electron volts. Dash-dot line, middle of first band; solid line, top of first band; dotted line, bottom of second band.

qualitative description.

Blount breakdown, which was discussed in the section MAGNETIC BREAKDOWN IN MODEL can also be examined for its usefulness in predicting sharp changes of behavior in the model. Figure 3 contains curves that show at which energies Blount breakdown is to be expected on the basis of equation (59) or (60). In examining Blount breakdown, changes must not really be sought in the behavior of states that are rather close to one another. Blount's criterion, as given by equation (60), actually states the breakdown occurs when E is "near" $(2V_0')^{1/2}/E_g^2$; therefore, states near this quantity must be compared with others rather well separated from them.

In order to test Blount breakdown in the model, a set of "D_N tested" eigenvalues (see appendix A) for a fixed value of H is required over a rather wide energy range. The results of the computations were such that such sets were available only for the well depth $V_0 = 5$ electron volts. Thus, figure 3(c) should be referred to in order to see where the states lie relative to the Blount line.

It can be seen from figure 3(d) that all the states shown in figures 5 to 9 are well below Blount breakdown. These figures, therefore, can furnish no information as to the validity of the Blount criterion for the model.

Figure 10 shows wave functions for a well depth of 5 electron volts for states rather well before, near, and after Blount breakdown. Figure 10(a) shows states for $V_0 = 5$ electron volts at $H = 3.8$ kilotesla ($V_0' = 0.1148$ ev). These states share a feature with those states in figures 5 to 9 of all being below Blount breakdown (see fig. 3(c)). As in the aforementioned figures, the states flanking the energy gap demonstrate distinctly different behaviors. (It should be noted, however, that the roles of the states have been reversed in comparison with the earlier figures. The significance of this reversal is not clear at present). Next, states at $H = 4.9$ kilotesla ($V_0' = 0.191$ ev) are shown in figure 10(b). From figure 3(c) it may be noted that the states flanking the gap, while still below Blount breakdown, are closer to it than the states in figure 10(a). The main feature of interest in this figure is that the difference between the flanking states is smaller than in figure 10(a). The amplitude of the state at the bottom of the second band is greater here and for $\lambda' = 1.5$ angstroms is quite comparable to that of the state at the top of the first band. The latter state, in turn, has a greater amplitude near the end of the chain than the state in figure 10(a). The transition is completed at $H = 5.8$ kilotesla ($V_0' = 0.268$ ev). As seen in figure 3(c), the Blount line passes through the gap at this field, so both flanking states are actually near Blount breakdown. These states are shown in figure 10(c). It may be noted there that the differences between the flanking states are greatly diminished in comparison with cases shown below the Blount line. Incidentally, the amplitudes of the flanking states are now in the same relative position as those at $V_0 = 10$ electron volts, which were all below Blount breakdown. Finally, figure 10(d) shows states past Blount breakdown.

Thus, it would appear that the periodic part of the potential exerts a strong influence on the system for states well below Blount breakdown, the states corresponding to the ones flanking the first gap in the zero-field band structure consistently exhibiting significantly different behavior. On the other hand, as Blount's criterion begins to be satisfied, the periodic potential has a much weaker effect, and the changes between states flanking the energy gap become far less pronounced.

The remaining type of breakdown, strong breakdown, has not been investigated in detail for reasons that would seem to be obvious. The strong breakdown line in figure 3, for the most part, involves states that lie so far above the bottom of the second band that they would lie in the continuum were it not for the box property of the chain. A few wave functions in this region were computed and showed only the typical behavior characteristic of "free particles in a box." These wave functions, therefore, would not appear to contribute markedly to an understanding of breakdown in the model.

SUMMARY OF RESULTS

A one-dimensional model has been examined in an attempt to follow magnetic breakdown in some detail. The model is that of an electron in a uniform magnetic field H_Z and a one-dimensional chain 20 atoms long of periodic square wells with infinite potential at each end. Exact solutions have been obtained for both the eigenvalues and the wave functions for arbitrary values of well depth, well width, atomic separation, and magnetic field strength. Computations have been carried out for several well depths from 1 to 10 electron volts and for several magnetic field strengths. Although the magnetic fields were of the order of tens of megagauss, it has proved possible to associate these states with corresponding zero-field states.

Three types of breakdown were considered for applicability to the model. The simplest type was one in which the magnitude of the magnetic part of the potential was equal to the depth of the "periodic" part of the potential. Another type was one in which the field was so large that the increase in the magnetic part of the potential over an atomic distance was equal to the well depth. The third type of breakdown examined was Blount breakdown in which $\hbar\omega_c E_F/E_g^2$ is compared with 1.

An examination of the wave functions for various conditions showed that below Blount breakdown the system is controlled by the periodic part of the potential and the accompanying band structure. The most persistently apparent characteristic of these results is that at a fixed magnetic field there is a sharp change in behavior of the wave functions in going from a state corresponding to the top of the first band in zero magnetic field to a state corresponding to the bottom of the second band in the zero-field situation. This behavior seems to admit an interpretation in terms of a change of orbits in k-space between states on either side of a Brillouin zone.

When the magnetic fields become large enough to cause the system to undergo Blount breakdown, the aforementioned differences between states flanking the zero-field energy gap become attenuated to a large extent. Consequently, in this case, the periodic part of the potential plays a far less decisive role in determining the behavior of the system.

Lewis Research Center
National Aeronautics and Space Administration
Cleveland, Ohio, October 1, 1964

APPENDIX A

DERIVATION OF EIGENVALUES

As mentioned in the section SOLUTION OF WAVE EQUATION, B_0^w is chosen as arbitrary. Then the requirements of continuity of $\lambda(x')$ and $(d/dx')\lambda(x')$ are satisfied by matching the wave function at every boundary. The boundary between the 0^{th} hill and the 0^{th} well occurs at $x' = w$. Thus,

$$\left[\lambda_0^w(x')\right]_{x'=w} = \left[\lambda_0^h(x')\right]_{x'=w} \tag{A1}$$

and

$$\left[\frac{d}{dx'}\lambda_0^w(x')\right]_{x'=w} = \frac{d}{dx'}\left[\lambda_0^h(x')\right]_{x'=w} \tag{A2}$$

Substituting equations (44) to (47) into equations (A1) and (A2) results in

$$B_0^w \cos wG_0^w = B_0^h \tag{A3}$$

and

$$-B_0^w G_0^w \sin wG_0^w = A_0^h \tag{A4}$$

Both equations (A3) and (A4) are independent of the value of g_0^h. The remainder of the matching equations are considered next. At the boundary between the n^{th} well and the n^{th} hill (this boundary is the right boundary of the well region and the left boundary of the hill region), $x' = na + w$ and it is therefore required that

$$\lambda_n^w(na + w) = \lambda_n^h(na + w) \tag{A5}$$

and

$$\frac{d}{dx'}\lambda_n^w(na + w) = \frac{d}{dx'}\lambda_n^h(na + w) \tag{A6}$$

By examining the form of $\lambda_n^w(x')$ and $\lambda_n^h(x')$ from equations (45) and (46), it is noted that $\lambda_n^w(x')$ involves functions of $x' - (na - w)$, whereas $\lambda_n^h(x')$ is expressed as a function of $x' - (na + w)$. Thus, $\lambda_n^w(na + w)$ will be a function of $2w$ and $\lambda_n^h(na + w)$ will be a function of 0. Therefore, the matching equations will take the form

$$\left.\begin{array}{lr} (A_n^w/G_n^w)\sinh 2wG_n^w + B_n^w \cosh 2wG_n^w & g_n^w < 0 \\ A_n^w(2w) + B_n^w & g_n^w = 0 \\ (A_n^w/G_n^w)\sin 2wG_n^w + B_n^w \cos 2wG_n^w & g_n^w > 0 \end{array}\right\} = B_n^h \tag{A7}$$

and

$$\left.\begin{array}{lr} A_n^w \cosh 2wG_n^w + B_n^w G_n^w \sinh 2wG_n^w & g_n^w < 0 \\ A_n^w & g_n^w = 0 \\ A_n^w \cos 2wG_n^w - B_n^w G_n^w \sin 2wG_n^w & g_n^w > 0 \end{array}\right\} = A_n^h \tag{A8}$$

Both equations (A7) and (A8) are independent of the value of g_n^h.

In a very similar way, the form of the matching equations at the boundary between the n^{th} well and the $n^{th} + 1$ well (where $x' = (n + 1)a - w$) can be readily expressed as

$$\left.\begin{array}{lr} (A_n^h/G_n^h)\sinh 2hG_n^h + B_n^h \cosh 2hG_n^h & g_n^h < 0 \\ A_n^h(2h) + B_n^h & g_n^h = 0 \\ (A_n^h/G_n^h)\sin 2hG_n^h + B_n^h \cos 2hG_n^h & g_n^h > 0 \end{array}\right\} = B_{n+1}^w \tag{A9}$$

$$\left.\begin{array}{lr} A_n^h \cosh 2hG_n^h + B_n^h G_n^h \sinh 2hG_n^h & g_n^h < 0 \\ A_n^h & g_n^h = 0 \\ A_n^h \cos 2hG_n^h - B_n^h G_n^h \sin 2hG_n^h & g_n^h > 0 \end{array}\right\} = A_{n+1}^w \tag{A10}$$

Both equations (A9) and (A10) are independent of the value of g_{n+1}^w. (The simple form of the right side of these equations is one of the main reasons for centering the wave functions as in eqs. (45) and (46)).

These equations represent all of the conditions except the matching at the last boundary in the chain. In the $(N + 1)^{th}$ hill, use must be made of equation (47) for (x') at $x' = Na + w$. This value of x' will make $\lambda_N^h(x')$ a function of $-2h$. Therefore, matching at this last boundary yields the following:

$$\frac{A_N^w}{G_N^w}\sinh 2wG_N^w + B_N^w\cosh 2wG_N^w = \left\{\begin{array}{ll} -\dfrac{A_N^h}{G_N^h}\sinh 2hG_N^h & g_N^h < 0 \\ -A_N^h(2h) & g_N^h = 0 \\ -\dfrac{A_N^h}{G_N^h}\sin 2hG_N^h & g_N^h > 0 \end{array}\right\} g_N^w < 0$$

$$A_N^w(2w) + B_N^w = \left\{\begin{array}{ll} -\dfrac{A_N^h}{G_N^h}\sinh 2hG_N^h & g_N^h < 0 \\ -A_N^h(2h) & g_N^h = 0 \\ -\dfrac{A_N^h}{G_N^h}\sin 2hG_N^h & g_N^h > 0 \end{array}\right\} g_N^w = 0 \tag{A11}$$

$$\frac{A_N^w}{G_N^w}\sin 2wG_N^w + B_N^w\cos 2wG_N^w = \left\{\begin{array}{ll} -\dfrac{A_N^h}{G_N^h}\sinh 2hG_N^h & g_N^h < 0 \\ -A_N^h(2h) & g_N^h = 0 \\ -\dfrac{A_N^h}{G_N^h}\sin 2hG_N^h & g_N^h > 0 \end{array}\right\} g_N^w > 0$$

$$A_N^w\cosh 2wG_N^w + B_N^wG_N^w\sinh 2wG_N^w = \left\{\begin{array}{ll} A_N^h\cosh 2hG_N^h & g_N^h < 0 \\ A_N^h & g_N^h = 0 \\ A_N^h\cos 2hG_N^h & g_N^h > 0 \end{array}\right\} g_N^w < 0$$

$$A_N^w = \left\{\begin{array}{ll} A_N^h\cosh 2hG_N^h & g_N^h < 0 \\ A_N^h & g_N^h = 0 \\ A_N^h\cos 2hG_N^h & g_N^h > 0 \end{array}\right\} g_N^w = 0 \tag{A12}$$

$$A_N^w\cos 2wG_N^w - B_N^wG_N^w\sin 2wG_N^w = \left\{\begin{array}{ll} A_N^h\cosh 2hG_N^h & g_N^h < 0 \\ A_N^h & g_N^h = 0 \\ A_N^h\cos 2hG_N^h & g_N^h > 0 \end{array}\right\} g_N^w > 0$$

In order to obtain the determinantal compatibility conditions from these equations, it will be convenient to introduce some notation that will enable the three possible expressions for the matched wave function (which depend on the values of g) to be condensed into a single expression.

A C preceding an A or B will denote the coefficient of that A or B in the appropriate matched wave function λ, and $C'A$ or $C'B$ will denote the coefficient of the A or B in the appropriate matched $d\lambda/dx'$. A subscript L or R on the C will denote whether the matching is at the left or right boundary, respectively, of the region in which the wave function is operating. Thus, w is the right boundary of the 0^{th} well and the left boundary of the 0^{th} hill, so that equations (A3) and (A4) can be written

$$B_0^w C_R B_0^w - B_0^h = 0 \tag{A13}$$

$$B_0^w C_R' B_0^w - A_0^h = 0 \tag{A14}$$

where

$$\left.\begin{aligned} C_R B_0^w &= \cos wG_0^w \qquad &\text{(A15)} \\ C_R' B_0^w &= -G_0^w \sin wG_0^w \qquad &\text{(A16)} \end{aligned}\right\} \quad g_0^w \text{ always} > 0$$

In a similar way, it is seen from equations (A7) and (A8) that it is possible to write

$$A_n^w C_R A_n^w + B_n^w C_R B_n^w - B_n^h = 0 \tag{A17}$$

$$A_n^w C_R' A_n^w + B_n^w C_R' B_n^w - A_n^h = 0 \tag{A18}$$

so that

$$C_R^{\stackrel{\bar{0}}{+}} A_n^w = \begin{cases} \sinh 2wG_n^w/G_n^w \\ 2w \\ \sin 2wG_n^w/G_n^w \end{cases} \tag{A19}$$

$$C_R^{\stackrel{\bar{0}}{+}} B_n^w = C_R'^{\stackrel{\bar{0}}{+}} A_n^w = \begin{cases} \cosh 2wG_n^w \\ 1 \\ \cos 2wG_n^w \end{cases} \tag{A20}$$

$$C_R'^{\overset{\bar{0}}{+}} B_n^w = \begin{cases} G_n^w \sinh 2wG_n^w \\ 0 \\ -G_n^w \sin 2wG_n^w \end{cases} \tag{A21}$$

The superscripts $\overset{\bar{0}}{+}$ on the C's refer to the sign of the appropriate g. Equations (A9) and (A10) may be written in the same way. Thus,

$$A_n^h C_R A_n^h + B_n^h C_R B_n^h - B_{n+1}^w = 0 \tag{A22}$$

$$A_n^h C_R' A_n^h + B_n^h C_R' B_n^h - A_{n+1}^w = 0 \tag{A23}$$

where

$$C_R^{\overset{\bar{0}}{+}} A_n^h = \begin{cases} \sinh 2hG_n^h / G_n^h \\ 2h \\ \sin 2hG_n^h / G_n^h \end{cases} \tag{A24}$$

$$C_R^{\overset{\bar{0}}{+}} B_n^h = C_R'^{\overset{\bar{0}}{+}} A_n^h = \begin{cases} \cosh 2hG_n^h \\ 1 \\ \cos 2hG_n^h \end{cases} \tag{A25}$$

$$C_R'^{\overset{\bar{0}}{+}} B_n^h = \begin{cases} G_n^h \sinh 2hG_n^h \\ 0 \\ -G_n^h \sin 2hG_n^h \end{cases} \tag{A26}$$

Finally, equations (A11) and (A12) become

$$A_N^w C_R A_N^w + B_N^w C_R B_N^w - A_N^h C_L A_N^h = 0 \tag{A27}$$

$$A_N^w C_R' A_N^w + B_N^w C_R' B_N^w - A_N^h C_L' A_N^h = 0 \tag{A28}$$

where $C_R A_N^w$, $C_R B_N^w$, $C_R' A_N^w$, and $C_R' B_N^w$ have the same form as equations (A19) and (A20) with $n = N$ and where

$$C_L^{\substack{-\\0\\+}} A_N^h = \begin{cases} -\sinh 2hG_N^h / G_N^h \\ \\ -2h \\ \\ -\sin 2hG_N^h / G_N^h \end{cases} \tag{A29}$$

$$C_L'^{\substack{-\\0\\+}} A_N^h = \begin{cases} \cosh 2hG_N^h \\ \\ 1 \\ \\ \cos 2hG_N^h \end{cases} \tag{A30}$$

The usual argument is now invoked, which says that if equations (A13), (A14), (A17), (A18), (A22), (A23), (A27), and (A28) are to hold simultaneously, then the determinant of all the coefficients must vanish. This is the determinantal compatibility condition that is being sought. Equation (A31) shows this determinant, which will be denoted by D_N. The columns are labeled according to the A or B whose coefficient appears in D_N. It will prove convenient to start with the equation for the last boundary and work toward the 0^{th} well.

$$\begin{array}{cccccccccc c}
A_N^h & A_N^w & B_N^w & A_{N-1}^h & B_{N-1}^h & A_{N-1}^w & B_{N-1}^w & \cdots & A_0^h & B_0^h & B_0^w \\
\hline
+C_L A_N^h & -C_R A_N^w & -C_R B_N^w & 0 & 0 & 0 & 0 & \cdots & 0 & 0 & 0 \\
+C_L' A_N^h & -C_R' A_N^w & -C_R' B_N^w & 0 & 0 & 0 & 0 & \cdots & 0 & 0 & 0 \\
0 & 0 & 1 & -C_R A_{N-1}^h & -C_R B_{N-1}^h & 0 & 0 & \cdots & 0 & 0 & 0 \\
0 & 1 & 0 & -C_R' A_{N-1}^h & -C_R' B_{N-1}^h & 0 & 0 & \cdots & 0 & 0 & 0 \\
0 & 0 & 0 & 0 & 1 & -C_R A_{N-1}^w & -C_R B_{N-1}^w & \cdots & 0 & 0 & 0 \\
0 & 0 & 0 & 1 & 0 & -C_R' A_{N-1}^w & -C_R' B_{N-1}^w & \cdots & 0 & 0 & 0 \\
\vdots & \vdots & \vdots & \vdots & \vdots & \vdots & \vdots & & \vdots & \vdots & \vdots \\
0 & 0 & 0 & 0 & 0 & 0 & 0 & \cdots & -C_R A_0^h & -C_R B_0^h & 0 \\
0 & 0 & 0 & 0 & 0 & 0 & 0 & \cdots & -C_R' A_0^h & -C_R' B_0^h & 0 \\
0 & 0 & 0 & 0 & 0 & 0 & 0 & \cdots & 0 & 1 & -\cos wG_0^w \\
0 & 0 & 0 & 0 & 0 & 0 & 0 & \cdots & 1 & 0 & G_0^w \sin wG_0^w
\end{array} \tag{A31}$$

The determinant D_N is $(4N + 2) \times (4N + 2)$. It will be evaluated in the usual way be expanding it in minors. By referring to (A31), it is seen that

$$D_N = C_L A_N^h \begin{vmatrix} -C_R' A_N^w & -C_R' B_N^w & 0 & 0 & 0 & 0 & \cdots & 0 & 0 & 0 \\ 0 & 1 & -C_R A_{N-1}^h & -C_R B_{N-1}^h & 0 & 0 & \cdots & 0 & 0 & 0 \\ 1 & 0 & -C_R' A_{N-1}^h & -C_R' B_{N-1}^h & 0 & 0 & \cdots & 0 & 0 & 0 \\ 0 & 0 & 0 & 1 & -C_R A_{N-1}^w & -C_R B_{N-1}^w & \cdots & 0 & 0 & 0 \\ 0 & 0 & 1 & 0 & -C_R' A_{N-1}^w & -C_R' B_{N-1}^w & \cdots & 0 & 0 & 0 \\ \vdots & \vdots & \vdots & \vdots & \vdots & \vdots & & \vdots & \vdots & \vdots \\ 0 & 0 & 0 & 0 & 0 & 0 & \cdots & -C_R A_0^h & -C_R B_0^h & 0 \\ 0 & 0 & 0 & 0 & 0 & 0 & \cdots & -C_R' A_0^h & -C_R' B_0^h & 0 \\ 0 & 0 & 0 & 0 & 0 & 0 & \cdots & 0 & 1 & -\cos wG_0^w \\ 0 & 0 & 0 & 0 & 0 & 0 & \cdots & 1 & 0 & G_0^w \sin wG_0^w \end{vmatrix}$$

$$- C_L' A_N^h \begin{vmatrix} -C_R A_N^w & -C_R B_N^w & 0 & 0 & 0 & 0 & \cdots & 0 & 0 & 0 \\ 0 & 1 & -C_R A_N^w & -C_R B_{N-1}^h & 0 & 0 & \cdots & 0 & 0 & 0 \\ 1 & 0 & -C_R' A_{N-1}^h & -C_R' B_{N-1}^h & 0 & 0 & \cdots & 0 & 0 & 0 \\ 0 & 0 & 0 & 1 & -C_R A_{N-1}^w & -C_R B_{N-1}^w & \cdots & 0 & 0 & 0 \\ 0 & 0 & 1 & 0 & -C_R' A_{N-1}^w & -C_R' B_{N-1}^w & \cdots & 0 & 0 & 0 \\ \vdots & \vdots & \vdots & \vdots & \vdots & \vdots & & \vdots & \vdots & \vdots \\ 0 & 0 & 0 & 0 & 0 & 0 & \cdots & -C_R A_0^h & -C_R B_0^h & 0 \\ 0 & 0 & 0 & 0 & 0 & 0 & \cdots & -C_R' A_0^h & -C_R' B_0^h & 0 \\ 0 & 0 & 0 & 0 & 0 & 0 & \cdots & 0 & 1 & -\cos wG_0^w \\ 0 & 0 & 0 & 0 & 0 & 0 & \cdots & 1 & 0 & G_0^w \sin wG_0^w \end{vmatrix} \tag{A32}$$

It may be observed that the determinants which are the coefficients of $C_L A_N^h$ and $C_L' A_N^h$, respectively, are identical except for their first rows. The coefficient of $C_L' A_N^h$ is denoted by S_N^w, while the coefficient of $C_L A_N^h$ is denoted by $\overline{S}_N^w$. An attempt at descriptive notation is being made here since S_N^w and $\overline{S}_N^w$ are, respectively, determinants in which the upper right terms are $-C_R A_N^w$ and $-C_R' A_N^w$. With this notation

$$D_N = \overline{S}_N^w C_L A_N^h - S_N^w C_L' A_N^h = 0 \tag{A33}$$

Now let $\bar{S}_N^w$ be reduced to see if a pattern can be found whereby the entire determinant can be evaluated readily. Expanding $\bar{S}_N^w$ by minors yields

$$\bar{S}_N^w = -C_R'A_N^w \begin{vmatrix} 1 & -C_RA_{N-1}^h & -C_RB_{N-1}^h & 0 & 0 & \cdots & 0 & 0 & 0 \\ 0 & -C_R'A_{N-1}^h & -C_R'B_{N-1}^h & 0 & 0 & \cdots & 0 & 0 & 0 \\ 0 & 0 & 1 & -C_RA_{N-1}^w & -C_RB_{N-1}^w & \cdots & 0 & 0 & 0 \\ 0 & 1 & 0 & -C_R'A_{N-1}^w & -C_R'B_{N-1}^w & \cdots & 0 & 0 & 0 \\ \vdots & \vdots & \vdots & \vdots & \vdots & & \vdots & \vdots & \vdots \\ 0 & 0 & 0 & 0 & 0 & \cdots & -C_RA_0^h & -C_RB_0^h & 0 \\ 0 & 0 & 0 & 0 & 0 & \cdots & -C_R'A_0^h & -C_R'B_0^h & 0 \\ 0 & 0 & 0 & 0 & 0 & \cdots & 0 & 1 & -\cos wG_0^w \\ 0 & 0 & 0 & 0 & 0 & \cdots & 1 & 0 & G_0^w \sin wG_0^w \end{vmatrix}$$

$$+ \begin{vmatrix} -C_R'B_N^w & 0 & 0 & 0 & 0 & \cdots & 0 & 0 & 0 \\ 1 & -C_RA_{N-1}^h & -C_RB_{N-1}^h & 0 & 0 & \cdots & 0 & 0 & 0 \\ 0 & 0 & 1 & -C_RA_{N-1}^w & -C_RB_{N-1}^w & \cdots & 0 & 0 & 0 \\ 0 & 1 & 0 & -C_R'A_{N-1}^w & -C_R'B_{N-1}^w & \cdots & 0 & 0 & 0 \\ \vdots & \vdots & \vdots & \vdots & \vdots & & \vdots & \vdots & \vdots \\ 0 & 0 & 0 & 0 & 0 & \cdots & -C_RA_0^h & -C_RB_0^h & 0 \\ 0 & 0 & 0 & 0 & 0 & \cdots & -C_R'A_0^h & -C_R'B_0^h & 0 \\ 0 & 0 & 0 & 0 & 0 & \cdots & 0 & 1 & -\cos wG_0^w \\ 0 & 0 & 0 & 0 & 0 & \cdots & 1 & 0 & G_0^w \sin wG_0^w \end{vmatrix} \qquad \text{(A34)}$$

Expanding each remaining determinant by minors again yields

$$\bar{S}_N^w = -C_R'A_N^w\bar{S}_{N-1}^h - C_R'B_N^wS_{N-1}^h \qquad \text{(A35)}$$

where S_{N-1}^h and $\bar{S}_{N-1}^h$ have a readily deducible connotation analogous to S_N^w and $\bar{S}_N^w$, respectively. It should be noted that the determinants S_{N-1}^h and $\bar{S}_{N-1}^h$ have a structure much like that of S_N^w and $\bar{S}_N^w$; they merely begin with $-C_RA_{N-1}^h$ and $-C_R'A_{N-1}^h$ instead of $-C_RA_N^w$ and $-C_R'A_N^w$, respectively, and are of dimension two less than S_N^w and $\bar{S}_N^w$.

Similarly, expanding S_N^w by minors twice yields

$$S_N^w = -C_R A_N^w \begin{vmatrix} 1 & -C_R A^h_{N-1} & -C_R B^h_{N-1} & 0 & 0 & \cdots & 0 & 0 & 0 \\ 0 & -C'_R A^h_{N-1} & -C'_R B^h_{N-1} & 0 & 0 & \cdots & 0 & 0 & 0 \\ 0 & 0 & 1 & -C_R A^w_{N-1} & -C_R B^w_{N-1} & \cdots & 0 & 0 & 0 \\ 0 & 1 & 0 & -C'_R A^w_{N-1} & -C'_R B^w_{N-1} & \cdots & 0 & 0 & 0 \\ \vdots & \vdots & \vdots & \vdots & \vdots & & \vdots & \vdots & \vdots \\ 0 & 0 & 0 & 0 & 0 & \cdots & -C_R A^h & -C_R B^h_0 & 0 \\ 0 & 0 & 0 & 0 & 0 & \cdots & -C'_R A^h_0 & -C'_R B^h_0 & 0 \\ 0 & 0 & 0 & 0 & 0 & \cdots & 0 & 1 & -\cos wG^w_0 \\ 0 & 0 & 0 & 0 & 0 & \cdots & 1 & 0 & G^w_0 \sin wG^w_0 \end{vmatrix}$$

$$+ \begin{vmatrix} -C_R B^w_N & 0 & 0 & 0 & 0 & \cdots & 0 & 0 & 0 \\ 1 & -C_R A^h_{N-1} & -C_R B^h_{N-1} & 0 & 0 & \cdots & 0 & 0 & 0 \\ 0 & 0 & 1 & -C_R A^w_{N-1} & -C_R B^w_{N-1} & \cdots & 0 & 0 & 0 \\ 0 & 1 & 0 & -C'_R A^w_{N-1} & -C'_R B^w_{N-1} & \cdots & 0 & 0 & 0 \\ \vdots & \vdots & \vdots & \vdots & \vdots & & \vdots & \vdots & \vdots \\ 0 & 0 & 0 & 0 & 0 & \cdots & -C_R A^h_0 & -C_R B^h_0 & 0 \\ 0 & 0 & 0 & 0 & 0 & \cdots & -C'_R A^h_0 & -C'_R B^h_0 & 0 \\ 0 & 0 & 0 & 0 & 0 & \cdots & 0 & 1 & -\cos wG^w_0 \\ 0 & 0 & 0 & 0 & 0 & \cdots & 1 & 0 & G^w_0 \sin wG^w_0 \end{vmatrix} \qquad \text{(A36)}$$

Thus,

$$S_N^w = -C_R A_N^w \bar{S}^h_{N-1} - C_R B_N^w S^h_{N-1} \qquad \text{(A37)}$$

Since the form of S^h_{N-1} and $\bar{S}^h_{N-1}$ is so similar to the form of S^w_N and $\bar{S}^w_N$, respectively, it is clear that a general procedure now exists for expanding D_N by minors in successive steps. Thus,

$$S_n^w = -C_R A_n^w \bar{S}^h_{n-1} - C_R B_n^w S^h_{n-1} \qquad \text{(A38)}$$

$$\bar{S}_n^w = -C'_R A_n^w \bar{S}^h_{n-1} - C'_R B_n^w S^h_{n-1} \qquad \text{(A39)}$$

and

$$S_n^h = -C_R A_n^h \bar{S}^w_n - C_R B_n^h S^w_n \qquad \text{(A40)}$$

$$\bar{S}_n^h = -C_R^{'}A_n^h\bar{S}_n^w - C_R^{'}B_n^hS_n^w \tag{A41}$$

The process continues in this fashion until S_0^h and $\bar{S}_0^h$ are reached. These have the special form indicated by the three columns and four rows in the lower right corner of all of the previous determinants. Thus,

$$S_0^h = \begin{vmatrix} -C_RA_0^h & -C_RB_0^h & 0 \\ 0 & 1 & -\cos wG_0^w \\ 1 & 0 & G_0^w \sin wG_0^w \end{vmatrix}$$

or

$$S_0^h = -C_RA_0^hG_0^w \sin wG_0^w + C_RB_0^h \cos wG_0^w \tag{A42}$$

and

$$\bar{S}_0^h = \begin{vmatrix} -C_R^{'}A_0^h & -C_R^{'}B_0^h & 0 \\ 0 & 1 & -\cos wG_0^w \\ 1 & 0 & G_0^w \sin wG_0^w \end{vmatrix}$$

so that

$$\bar{S}_0^h = -C_R^{'}A_0^hG_0^w \sin wG_0^w + C_R^{'}B_0^h \cos wG_0^w \tag{A43}$$

Actually, equations (A42) and (A43) can be made consistent with equations (A38) to (A41) if the following identification is made:

$$S_0^w = -\cos wG_0^w \tag{A44}$$

$$\bar{S}_0^w = G_0^w \sin wG_0^w \tag{A45}$$

In going over what has been done, it may be noted that a procedure has been developed for evaluating D_N by starting at the lower right corner and working toward the upper left corner. Since this is a somewhat unusual procedure, there may be some merit in summarizing it.

The terms V_0 and $V_0^{'}$ are fixed and then the eigenvalue for such a $V(x')$ is determined as follows: A trial value of E is chosen, G_0^w is evaluated, and then S_0^w and $\bar{S}_0^w$ are obtained from equations (A44) and (A45).

These values are then substituted into equations (A40) and (A41) and by successive application of equations (A38) to (A41) all of the S's and $\overline{S}$'s through S_N^w and $\overline{S}_N^w$ are obtained. Then the quantity in equation (A33) is found, $D_N = C_L A_N^h \overline{S}_N^w - C_L' A_N^h S_N^w$, and a decision is made as to whether it is sufficiently close to zero. If it is, the trial value of E is chosen to be an eigenvalue for the fixed V_0 and V_0' assumed. If the D_N so formed is not close enough, the entire procedure is repeated with a new trial value of E until a sufficiently small D_N is obtained. Actually, there are many eigenvalues for each given V_0 and V_0', as can be seen from figures 3 and 4.

It is readily seen that for odd $\lambda(x')$ the only change that need be made in the aforementioned procedure is that $\lambda_0^w(x') = A_0^w \sin G_0^w x'/G_0^w$ and that S_0^w and $\overline{S}_0^w$ will be given by

$$S_0^w = -\sin wG_0^w/G_0^w \tag{A46}$$

$$\overline{S}_0^w = -\cos wG_0^w \tag{A47}$$

APPENDIX B

DERIVATION OF WAVE FUNCTION

Once having obtained an eigenvalue, the unnormalized wave function for that eigenvalue is readily obtained from the matching equations shown in appendix A. Since B_0^w is going to be used as the arbitrary amplitude, there immediately results (from eqs. (A13) and (A14))

$$A_0^h = B_0^w C_R' B_0^w = (-G_0^w \sin wG_0^w)B_0^w$$

$$B_0^h = B_0^w C_R B_0^w = (\cos wG_0^w)B_0^w$$

Thus,

$$A_0^h/B_0^w = -G_0^w \sin wG_0^w \tag{B1}$$

$$B_0^h/B_0^w = \cos wG_0^w \tag{B2}$$

Equations (B1) and (B2) are then substituted into equations (A22) and (A23) with $n = 0$, the results substituted into equations (A17) and (A18), and these equations used successively until A_N^w/B_0^w and B_N^w/B_0^w are obtained. At this point A_N^h can be obtained from equations (A27) or (A30). If the value of D_N used to find the eigenvalue was sufficiently small, then the values of A_N^h/B_0^w obtained from these two equations will be close enough. If D_N were actually 0, then the values of A_N^h using the two equations would be identical.

The set of coefficients of $\lambda(x')$ in each interval having been obtained, the (unnormalized) wave function at any given value of x' can be computed. The normalization of $\lambda(x')$ would allow a comparison to be made between the relative probability densities of eigenfunctions belonging to different eigenvalues in any region. This procedure is carried out in appendix C.

For odd $\lambda(x')$, A_0^w will be used as the arbitrary amplitude, and instead of equations (B1) and (B2), there will be

$$A_0^h/A_0^w = \cos(wG_0^w) \tag{B3}$$

$$B_0^h/A_0^w = \sin(wG_0^w)/G_0^w \tag{B4}$$

The remainder of the procedure is unchanged.

APPENDIX C

NORMALIZATION OF WAVE FUNCTION

The wave functions will be normalized in the usual way; that is, the otherwise arbitrary constant B_0^w is determined so that

$$\int_{-\infty}^{\infty} |\lambda(x')|^2 \, dx' = 1 \tag{C1}$$

As has been seen, $\lambda(x')$ assumes a different form in each interval and, within a given interval, for each sign of the appropriate g for that interval. Whether the solution be even or odd, it will still be true that

$$\int_{-\infty}^{\infty} |\lambda(x')|^2 \, dx' = 2 \int_{0}^{\infty} |\lambda(x')|^2 \, dx' \tag{C2}$$

Furthermore, the right side may be broken up in the following way (taking account of the fact that $\lambda(x') = 0$, $x' \geq (N + 1)a - w$):

$$\int_{0}^{\infty} |\lambda(x')|^2 \, dx' = \left\{ \int_{0}^{w} + \sum_{n=0}^{N} \left[\int_{na+w}^{(n+1)a-w} \right] + \sum_{n=1}^{N} \left(\int_{na-w}^{na+w} \right) \right\} |\lambda(x')|^2 \, dx' \tag{C3}$$

The $\lambda(x')$ in each interval may be replaced by its special form as given in equations (45) and (46), and the normalization condition obtained in the form

$$\frac{1}{2} = \int_{0}^{w} |\lambda_0^w(x')|^2 \, dx' + \sum_{n=0}^{N} \left[\int_{na+w}^{(n+1)a-w} |\lambda_n^h(x')|^2 \, dx' \right] + \sum_{n=1}^{N} \left[\int_{na-w}^{na+w} |\lambda_n^w(x')|^2 \, dx' \right] \tag{C4}$$

In appendix B, a procedure was displayed for obtaining each of the coefficients A_n^w, B_n^w, A_n^h, and B_n^h in terms of B_0^w. It is clear then that, if all coefficients be expressed in terms of B_0^w, the wave function in each interval can be written as $B_0^w f_n^w(x')$ or $B_0^w f_n^h(x')$, where $f_n^w(x')$ and $f_n^h(x')$ are the forms of $\lambda_n^w(x')$ and $\lambda_n^h(x')$, respectively, after the A_n^w, B_n^w, A_n^h, and B_n^h have been so expressed.

If

$$F_0^w = \int_0^w |f_0^w(x')|^2 \, dx' \tag{C5}$$

$$F_n^h = \int_{na+w}^{(n+1)a-w} |f_n^h(x')|^2 \, dx' \tag{C6}$$

and

$$F_n^w = \int_{na-w}^{na+w} |f_n^w(x')|^2 \, dx' \tag{C7}$$

there results at once (using eq. (C4))

$$|B_0^w|^2 = \frac{1/2}{F_0^w + \sum_{n=0}^{N} F_n^h + \sum_{n-1}^{N} F_n^w} \tag{C8}$$

The remaining task is to find the F's. The form of $f_0^w(x')$ is always $\cos G_0^w x'$; therefore,

$$F_0^w = \int_0^w \cos^2 G_0^w x' \, dx' = \frac{1}{2}\left(w + \frac{\sin 2wG_0^w}{2G_0^w}\right) \tag{C9}$$

Each of the remaining F's may have several forms depending on the value of g that goes with the f in question. It is readily ascertained that the change of variables

$$\nu = x' - (na - w) \text{ for a well region} \tag{C10}$$

$$\mu = x' - (na + w) \text{ for a hill region} \tag{C11}$$

will simplify the algebra involved in evaluating the F's. With these changes, there remains only the evaluation of the following integrals:

$$\frac{1}{(G_n^h)^2}\int_0^{2h} \sinh^2 G_n^h\mu \, d\mu = \frac{h}{(G_n^h)^2}\left(\frac{\sinh 4hG_n^h}{4hG_n^h} - 1\right) \tag{C12a}$$

$$\int_0^{2h} \cosh^2 G_n^h\mu \, d\mu = h\left(\frac{\sinh 4hG_n^h}{4hG_n^h} + 1\right) \tag{C12b}$$

$$\frac{1}{G_n^h}\int_0^{2h} \sinh G_n^h\mu \cosh G_n^h\mu \, d\mu = \frac{1}{2G_n^h}\int_0^{2h} \sinh 2G_n^h\mu \, d\mu$$

$$= \frac{1}{4(G_n^h)^2}\left(\cosh 4hG_n^h - 1\right) \tag{C12c}$$

$$\int_0^{2h} \mu^2 \, d\mu = \frac{(2h)^3}{3} \tag{C13a}$$

$$\int_0^{2h} d\mu = 2h \tag{C13b}$$

$$\int_0^{2h} \mu \, d\mu = \frac{(2h)^2}{2} \tag{C13c}$$

$$\frac{1}{(G_n^h)^2}\int_0^{2h} \sin^2 G_n^h\mu \, d\mu = \frac{h}{(G_n^h)^2}\left(1 - \frac{\sin 4hG_n^h}{4hG_n^h}\right) \tag{C14a}$$

$$\int_0^{2h} \cos^2 G_n^h\mu \, d\mu = h\left(1 + \frac{\sin 4hG_n^h}{4hG_n^h}\right) \tag{C14b}$$

$$\frac{1}{G_n^h}\int_0^{2h} \sin G_n^h\mu \cos G_n^h\mu \, d\mu = \frac{1}{2G_n^h}\int_0^{2h} \sin 2G_n^h\mu \, d\mu$$

$$= \frac{1}{4(G_n^h)^2}\left(1 - \cos 4hG_n^h\right) \tag{C14c}$$

Equations (C12) to (C14) are the forms involved when g_n^h is negative, zero, and positive, respectively. Corresponding well integrals are exactly the same with w replacing h each time the latter occurs.

If the α's and β's are defined as the ratios of the A's and B's to B_0^w so that

$$\alpha_n^w B_0^w = A_n^w \tag{C15}$$

$$\beta_n^w B_0^w = B_n^w \tag{C16}$$

$$\alpha_n^h B_0^w = A_n^h \tag{C17}$$

$$\beta_n^h B_0^w = B_n^h \tag{C18}$$

then

$$F_n^h = |\alpha_n^h|^2[a] + |\beta_n^h|^2[b] + \left(\alpha_n^{h*}\beta_n^h + \alpha_n^h\beta_n^{h*}\right)[c] \tag{C19}$$

where [a], [b], and [c] are obtained from (C12), (C13), or (C14) depending on g_n^h.

Similarly,

$$F_n^w = |\alpha_n^w|^2[a] + |\beta_n^w|^2[b] + \left(\alpha_n^{w*}\beta_n^w + \alpha_n^w\beta_n^{w*}\right)[c] \tag{C20}$$

where [a], [b], and [c] are obtained from the equations corresponding to (C12), (C13), and (C14), respectively, for a well region.

By choosing the forms in equations (45) and (46) as has been done, all of the A's and B's will be real (and thus also the α's and β's). Then equations (C19) and (C20) may be written

$$F_n^h = (\alpha_n^h)^2[a] + (\beta_n^h)^2[b] + 2\alpha_n^h\beta_n^h[c] \tag{C21}$$

$$F_n^w = (\alpha_n^w)^2[a] + (\beta_n^w)^2[b] + 2\alpha_n^w\beta_n^w[c] \tag{C22}$$

Now F_n^h and F_n^w can be written in full:

$$
F_n^{h\overset{\bar{0}}{+}} = \begin{cases}
\dfrac{h}{(G_n^h)^2}\left(\dfrac{\sinh 4hG_n^h}{4hG_n^h} - 1\right)\left(\alpha_n^h\right)^2 + h\left(\dfrac{\sinh 4hG_n^h}{4hG_n^h} + 1\right)\left(\beta_n^h\right)^2 \\
\qquad + \dfrac{1}{2\left(G_n^h\right)^2}\left(\cosh 4hG_n^h - 1\right)\left(\alpha_n^h\beta_n^h\right) \\[2ex]
\dfrac{(2h)^3}{3}(\alpha_n^h)^2 + (2h)(\beta_n^h)^2 + (2h)^2(\alpha_n^h\beta_n^h) \\[2ex]
\dfrac{h}{\left(G_n^h\right)^2}\left(1 - \dfrac{\sin 4hG_n^h}{4hG_n^h}\right)\left(\alpha_n^h\right)^2 + h\left(1 + \dfrac{\sin 4hG_n^h}{4hG_n^h}\right)\left(\beta_n^h\right)^2 \\
\qquad + \dfrac{1}{2\left(G_n^h\right)^2}\left(1 - \cos 4hG_n^h\right)\left(\alpha_n^h\beta_n^h\right)
\end{cases} \tag{C23}
$$

$$
F_n^{w\overset{\bar{0}}{+}} = \begin{cases}
\dfrac{w}{\left(G_n^w\right)^2}\left(\dfrac{\sinh 4wG_n^w}{4wG_n^w} - 1\right)\left(\alpha_n^w\right)^2 + w\left(\dfrac{\sinh 4wG_n^w}{4wG_n^w} + 1\right)\left(\beta_n^w\right)^2 \\
\qquad + \dfrac{1}{2\left(G_n^w\right)^2}\left(\cosh 4wG_n^w - 1\right)\left(\alpha_n^w\beta_n^w\right) \\[2ex]
\dfrac{(2w)^3}{3}\left(\alpha_n^w\right)^2 + (2w)\left(\beta_n^w\right)^2 + (2w)^2\left(\alpha_n^w\beta_n^w\right) \\[2ex]
\dfrac{w}{\left(G_n^w\right)^2}\left(1 - \dfrac{\sin 4wG_n^w}{4wG_n^w}\right)\left(\alpha_n^w\right)^2 + w\left(1 + \dfrac{\sin 4wG_n^w}{4wG_n^w}\right)\left(\beta_n^w\right)^2 \\
\qquad + \dfrac{1}{2\left(G_n^w\right)^2}\left(1 - \cos 4wG_n^w\right)\left(\alpha_n^w\beta_n^w\right)
\end{cases} \tag{C24}
$$

This completes the normalization. All of the quantities needed in equations (C8) are given by equations (C21), (C22), and (C9). If they be substituted in the right side of (C8) and the square root of the result taken, then the value of B_0^w so obtained will cause equation (C1) to be satisfied.

It should be noted that the results hold both for even and odd eigenfunctions, the only differences between these cases being that, first, a coefficient other than B_0^w will have to be chosen as arbitrary (since $\lambda_0^w(x')$ will be of the form $A_0^w \sin G_0^w x'/G_0^w$), which will make F_0^w take the form

$$F_0^w = \frac{w}{\left(G_0^w\right)^2}\left(1 - \frac{\sin 2wG_0^w}{2wG_0^w}\right) \tag{C25}$$

Secondly, the resulting α's and β's will be different for odd $\lambda(x')$.

APPENDIX D

FORTRAN IV PROGRAM FOR COMPUTATIONS OF EIGENVALUES

General Description

This program written in Fortran IV language (actually a converted Fortran II program) was used to compute the eigenvalues shown in figures 3 and 4. It is arranged to operate with the Lewis Research Center 7094 monitor system. It consists of a main routine and four subroutines. The main routine and the first subroutine are also used in the program to compute the wave functions.

Before listing the individual routines, it will be useful to note the following:

By using equation (56), n_{SB} may be written

$$n_{SB} = \frac{V_0}{2V_0'} \tag{D1}$$

so that

$$(V_M)_{SB} = n_{SB}^2 V_0' = \frac{V_0}{(2V_0')^2} V_0' \tag{D2}$$

As indicated in the section RESULTS AND DISCUSSION, the computations have been carried out to values 50-percent greater than $(V_M)_{SB}$. Thus, the computations are carried out to a value of H large enough to make $V_M(x') = 3(V_M)_{SB}/2$ or

$$\frac{3}{2}\left(\frac{V_0}{2V_0'}\right)^2 V_0' = N^2 V_0' \tag{D3}$$

from which a maximum value of V_0' was chosen. Thus,

$$(V_0')_{max} = \frac{\sqrt{3/2}\, V_0}{2N} \tag{D4}$$

Normally, this quantity was computed by the first subroutine VOPFIX for each value of V_0, and then computations were made for various multiples of $(1/8)^{th}$ of this value. For some purposes, computations were desired for a fixed $(V_0')_{max}$ for several values of V_0 (see fig. 4). This procedure was then not suitable, and $(V_0')_{max}$ was read into MAIN and remained unchanged for all of the values of V_0 set by MAIN.

A list of the routines and a short description of their primary functions follows.

MAIN determines what is to be computed (eigenvalues or wave functions) and stores the values of the parameters to be used by the subroutines in computing the eigenvalues.

Subroutine VOPFIX fixes the value of $V_M(x')$ to be used in the computations.

Subroutine EVFIND sets limits on search for eigenvalues, stores the eigenvalues found by other subroutines, and prints and/or punches the eigenvalues on sheets and/or cards.

Subroutine ZERO locates changes in sign of the determinant D_N as trial values for E are stepped, tests it for closeness to zero, and returns values of D_N and roots found to EVFIND.

Subroutine CALC computes value of D_N for trial values of E given to it by ZERO and returns value of D_N to ZERO.

Details of Individual Routines

MAIN provides needed flexibility in the computations. Desired values of N, w, h, a, and V_0 as well as the number of different values of V_0 in a given run are fixed first. Then the following options are decided:

VPSLCT determines whether the value of $V_M(x')$ will be computed by VOPFIX or set in MAIN.

EVSKIP determines whether eigenvalues or wave functions will be computed.

EVODD determines whether even or odd solutions are to be used in the computations. If it is decided to compute eigenvalues, then DWRITE determines whether or not each computed value of D_N will be printed out along with the trial value of E.

Next, various quantities are read in that determine the starting trial value to be used for E, the amount by which subsequent trial values are to be stepped, and the quantities to be used to determine whether the computed value of D_N is close enough to zero to permit the corresponding trial value of E to be accepted as an eigenvalue. Control is then transferred to a DO-loop that sets values of V_0 after which the program is terminated. That portion of MAIN used to compute the wave functions will be described in appendix E.

Subroutine VOPFIX, like MAIN, is used in computing wave functions as well as eigenvalues. Primarily, it sets specific values for V_0'. Secondarily, it computes the corresponding values for H in kG as well as the number of the atoms in the chain at which weak breakdown and strong breakdown occur. If EVSKIP was not equal to 2 in MAIN, then VOPFIX will call EVFIND.

It should be noted that a dummy subroutine NORMAL must be included in the deck when computing eigenvalues or the program will not run.

Subroutine EVFIND sets the starting value of E at which the search for eigenvalues is to begin and the maximum value for E at which the search is to terminate. When an E and its corresponding DN value are received, both are stored, a new starting value is chosen to be given to ZERO, and the process is continued until all the eigenvalues in the desired range have been found. All of the eigenvalues and the corresponding values of DN are then printed. Those eigenvalues for which the DN's are sufficiently close to zero are printed again separately. These latter eigenvalues are also punched out on IBM cards for use as input data in computing wave functions.

Subroutine ZERO sends the starting value of E obtained from EVFIND to CALC, which sends back the corresponding value of DN. The value of E is then increased by an amount set in MAIN and called STEP. This new value of E is again sent to CALC, which again sends back the corresponding DN. The entire process is continued until the sign of the DN that is sent back to ZERO changes from the sign of the last DN sent. At this point, a linear interpolation procedure begins and continues until $|DN|$ is smaller than an amount set in MAIN and called DTEST or until the amount by which the linear interpolation changes E is smaller than another quantity set in MAIN called PRECSN. When either of these two events occurs, the last values of E and DN are returned to EVFIND along with an indication (by means of sense lights) of which of the two events characterizes the particular pair of values of E and DN.

Each trial value of E along with the corresponding value of DN will be printed or not in accordance with the value of DWRITE that was set in MAIN.

Subroutine CALC utilizes the procedure indicated in appendix A to compute the value of DN when all of the parameters are fixed. Both even and odd solutions can be used in this subroutine.

Input Data

Units for the input data are the following: energy, electron volts; length, angstroms; magnetic field strength, kilogauss.

The data are input from tape 5. The names of the quantities for which the data are used together with a description of the actual use are now listed. The subroutines in which these quantities are used follow each description.

N number of atoms in positive half of chain (MAIN, VOPFIX, EVFIND, CALC)

W width of well portion in one period of $V_P(x')$ (MAIN, CALC)

H width of hill portion in one period of $V_P(x')$ (MAIN, CALC)

A distance of atomic separation (MAIN, VOPFIX, CALC)

KI beginning value of cycle of values of V_0 set in MAIN

KF largest value in cycle of values of V_0

KS step in values of cycle of values of V_0

VPSLCT 1, has MAIN fix V_0'; 2, has VOPFIX fix V_0' (MAIN, VOPFIX)

VPCHS value of V_0' given to MAIN (this card omitted if VPSLCT is 2) (MAIN, VOPFIX)

KIP beginning value of multiple of fractional value of $(V_0')_{max}$ used in VOPFIX to set values of V_0' (MAIN, VOPFIX)

KFP final value of preceding description

KSP step in value of preceding description

EVSKIP 1, does not compute eigenvalues; 2, does compute eigenvalues (MAIN, VOPFIX)

EVODD 1, computes even eigenvalues; 2, computes odd eigenvalues (MAIN, CALC)

DWRITE 1, values of DN printed in ZERO; 2, values of DN not printed in ZERO

XSTART beginning trial value of E in a set of computations seeking zero value of DN (MAIN, EVFIND, ZERO)

STEP value by which each successive trial value of E is stepped in process described previously (MAIN, EVFIND, ZERO)

PRECSN minimum interval of change from one trial value of E to another interpolated one that allows interpolation procedure to proceed (MAIN, ZERO)

DTEST maximum absolute value of DN that permits the eigenvalue to be used in computing wave functions (MAIN, ZERO)

XTEST minimum interval of change from one trial value of E to another interpolated one that allows ZERO to keep searching; if change is smaller than this and DN is less than DTEST, trial value is suitable for use in computing wave function; if DN is still larger than DTEST, search stops but the last trial value of E is unsuitable for use in wave function computations (MAIN, CALC)

A listing of the subroutines used in computing the eigenvalues follows.

```
$IBFTC MAIN     DECK
      DIMENSION JDO(100)
      DOUBLE PRECISION XSTART,STEP,XMAX,PRECSN,DTEST,XTEST
      DOUBLE PRECISION W,H,A,VO,VPCHS
      INTEGER XDSIZE,EVSKIP,DWRITE,EVODD,VPSLCT
      COMMON COM
      EQUIVALENCE (A,COM(1)),(W,COM(3)),(H,COM(5)),(VO,COM(7)),
     1(N,COM(16)),(XSTART,ESTART,COM(11)),(VPSLCT,COM(330)),
     2(DWRITE,COM(796)),(KIP,COM(13)),(KFP,COM(14)),(KSP,COM(15)),
     3(NI,COM(17)),(NF,COM(18)),(NS,COM(19)),(EVODD,COM(329)),
     4(EVSKIP,COM(223)),(JEV,COM(224)),(JDO,COM(225)),(KPLOT,COM(574)),
     5(STEP,COM(797)),(PRECSN,COM(799)),(XMAX,EMAX,COM(801)),
     6(DTEST,COM(803)),(VPCHS,COM(331)),(XDSIZE,COM(807)),
     7(XTEST,COM(811)),(LTM,COM(814)),(LTN,COM(815)),(KN,COM(816)),
     8(KSX,COM(817)),(KSY,COM(818)),(FX,COM(819)),(DX,COM(820)),
     9(FY,COM(821)),(DY,COM(822))
    1 READ  (5,71)N
   71 FORMAT(I4)
      READ  (5,72)W,H,A
   72 FORMAT(3D10.3)
      READ  (5,75)KI,KF,KS
   75 FORMAT(3I4)
C VPSLCT = 1,2 HAS MAIN,VOPFIX CHOOSE VOP
      READ (5,71) VPSLCT
      IF (VPSLCT.EQ.2) GO TO 6
      READ (5,78) VPCHS
   78 FORMAT (D15.8)
    6 READ  (5,75)KIP,KFP,KSP
C EVSKIP = 1,2 MEANS WAVE FUNCTION,EV CALCULATED, RESPECTIVELY
      READ(5,74)EVSKIP,JEV
   74 FORMAT(2I4)
      READ (5,71) EVODD
C EVODD =1,2 GIVES EVEN,ODD SOLUTIONS,RESPECTIVELY
      WRITE (6,62) (N,W,H,A,KI,KF,KS,KIP,KFP,KSP,EVODD,EVSKIP)
   62 FORMAT(1HK,10X,2HN=I2,2X,2HW=F4.2,2X,2HH=F4.2,2X,2HA=F4.2,2X,
     19HKI,KF,KS=3I3,14H, KIP,KFP,KSP=3I3,8H, EVODD=I2,9H, EVSKIP=I2)
      IF (EVSKIP.EQ.1)  GO TO 4
      READ (5,71)DWRITE
C DWRITE =1 WRITES DN
      READ  (5,73)XSTART,STEP
   73 FORMAT(2D11.4)
      READ  (5,77)PRECSN,DTEST ,XTEST
   77 FORMAT(3D11.4)
      WRITE(6,63)(DWRITE,XSTART,STEP,PRECSN,DTEST,XTEST)
   63 FORMAT(1HK,10X,7HDWRITE=I2,2X,12HXSTART,STEP=2D12.4,
     12X,19HPRECSN,DTEST,XTEST=3D12.4)
      GO TO 5
    4 READ  (5,75)NI,NF,NS
      READ  (5,76)JDO
   76 FORMAT (70I1/30I1)
C KPLOT = 1,2 MEANS PLOT MADE, SKIPPED ,RESPECTIVELY
      READ (5,71) KPLOT
      IF (KPLOT.EQ.2)  GO TO 5
C NO OF POINTS IS = TO THE VALUE OF XDSIZE
      READ (5,71) XDSIZE
C LTM SPECIFIES NUMBER  LINE SPACES BETWEEN GRID LINES
C LTN SPECIFIES NUMBER OF PRINT SPACES BETWEEN GRID LINES
C KN IS THE NUMBER OF CURVES
C EXP(KSX,KSY -6) TIMES FX,FY OR TIMES DX,DY = ACTUAL STARTING VALUES
C OR CHANGES IN GRID VALUES
      READ (5,51) LTM,LTN,KN,KSX,KSY
   51 FORMAT (5I4)
C FX USED TO SPECIFY STARTING VALUE OF VERTICAL SCALE
C DX USED TO SPECIFY  CHANGE IN VERTICAL GRID VALUES EACH LINE SPACE
C FY USED TO SPECIFY STARTING VALUE OF  HORIZONTAL SCALE
C DY USED TO SPECIFY  CHANGE IN HORIZONTAL GRID VALUES EACH PRINT SPACE
      READ (5,52) FX,DX,FY,DY
   52 FORMAT (4F8.3)
    5 IF (KI.EQ.0) GO TO 11
      DO 10 I= KI,KF,KS
    2 VO=I
   10 CALL VOPFIX
      GO TO 12
   11 VO = 0.0D0
      CALL VOPFIX
   12 STOP
      END
```

```
      SUBROUTINE VOPFIX
C GIVES CPTICN OF NOT CALCULATING EV
      DOUBLE PRECISICN W,H,A,VO,VOP,EV,VPCHS,XN,VPINT,BVOP,C
      INTEGER VPSLCT,EVSKIP
      CCMMON CCM
      EQUIVALENCE (A,COM(1)),(W,COM(3)),(H,COM(5)),(VO,COM(7)),
     1(N,COM(16)),(VCP,COM(325)),(VPSLCT,COM(330)),(VPCHS,COM(331)),
     2(DWRITE,COM(796)),(KIP,COM(13)),(KFP,COM(14)),(KSP,COM(15)),
     3(EVSKIP,COM(223)),(JEV,COM(224))
      IF (KIP.GT.0) GO TO 1
      VOP = 0.D0
      WRITE (6,63)
   63 FORMAT ( 1HK,5X,6HVOP=0,3X,5HHM=0,3X,21HNO MAGNETIC BREAKDOWN/1HK)
      GO TO (16,17),EVSKIP
   16 DO 18 J2 =1,JEV
      READ (5,71) EV
      CALL NCRMAL(EV)
   18 CONTINUE
      GO TO 15
   17 CALL EVFINC
      GO TC 15
    1 XN = N
      VPINT = KFP
      BVCP = VC*CSQRT(1.5D0)/(2.0D0*XN*VPINT)
    2 CH = 8.793984E-12
      DO 14 J= KIP,KFP,KSP
      C = J
      GO TO (19,3),VPSLCT
   19 VOP = VPCHS
      GC TO 20
    3 VCP = C*BVCP
   20 HM= SQRT(VCP/CH)/A
    9 WRITE (6,62)VO,VOP,HM
   62 FORMAT(1HK,5X,3HVO=F5.1,2X,4HVOP=F5.4,16X,3HHM=,1PE9.3,/1HK)
      GC TO (11,13),EVSKIP
   11 JEV =JEV
      DO 12 J1= 1,JEV
      READ  (5,71)EV
   71 FORMAT(D23.16)
      CALL NCRMAL(EV)
   12 CONTINUE
      GO TO 14
   13 CALL EVFINC
   14 CONTINLE
   15 RETURN
      END
```

```
      SUBROUTINE EVFIND
      DOUBLE PRECISION E,CN,ROOT,XSTART,XMAX,PRECSN,XBEGIN,ROOT1
      DOUBLE PRECISICN EV,EV1,DEV,DEV1,W,H,A,VO,VOP,XTEST
      DIMENSION EV(100),EV1(100),DEV(100),DEV1(100)
      COMMON COM
      EQUIVALENCE (A,COM(1)),(W,COM(3)),(H,COM(5)),(VO,COM(7)),
     1(N,CCM(16)),(VCP,COM(325)),(ROOT,COM(9)),(XSTART,ESTART,COM(11)),
     2(NEV,COM(20)),(EV,COM(21)),(E,X,COM(327)),(XTEST,COM(811)),
     3(STEP,COM(797)),(PRECSN,COM(799)),(XMAX,EMAX,COM(801)),
     4(DTEST,COM(803)),(DN,CCM(805)),(XBEGIN,COM(809))
      DO 6 J=1,1CO
      EV(J) = 0. DO
      DEV(J) = 0.0D0
      DEV1(J) = 0.0D0
    6 EV1(J) = 0.D0
    1 XN = N
      IF (VO.EQ.0.0D0) GO TO 25
    2 BEMAX= XN*VO*SQRT(1.5)/2.0
      IF (BEMAX-VO) 3,3,4
    3 EMAX = VC + 0.5
      GO TO 5
    4 EMAX = BEMAX + 0.5
      GO TO 5
   25 XMAX = 25.0D0
    5 XBEGIN = XSTART
      NEV = 0
      DO 15 J= 1,100
    7 CALL ZERO
C SENSE LIGHT 1 CN IF NO ROOT FOUND FOR X .GE. EMAX
      CALL SLITET(1,KOOOFX)
       GO TO(8,9),KOOOFX
    8 NEV = NEV +1
      EV(NEV) = C. DO
      DEV (NEV) = 0.0D0
      EV1(J) = 0.0D0
      DEV1(J) = 0.0D0
      GO TO 16
    9 IF (J.GT.1) GO TO 11
   10 EV1(J) = RCOT
      DEV1(J) = CN
C SLITE 3 ON IF RCOT CANNOT PASS DN TEST
      CALL SLITET(3,K)
      GO TO (19,18),K
C NEV = NUMBER OF  EVS WHICH ARE CN TESTED
   18 NEV = NEV +1
      EV(NEV) = RCOT
      DEV(NEV) = DN
   19 ROOT1 = ROOT
      GO TO 14
   11 IF (ROOT .GE.EMAX) GO TO 16
   12 IF(DABS(ROOT - ROOT1).GT. PRECSN) GO TO 10
      CALL SLITET(3,K)
      GO TO (13,22),K
   22 IF (NEV.GT.0) GO TO 21
      NEV = NEV + 1
   21 EV(NEV) = RCOT
      DEV(NEV) = CN
   13 XBEGIN = RCOT + STEP
      GO TO 7
   14 XBEGIN = RCOT
   15 CONTINUE
   16 WRITE (6,64) VO,VOP
   64 FORMAT (1HK,10X,3HVO=F4.1,4X,4HVOP=F8.4/1HK)
      WRITE(6,61) (EV1(I),DEV1(I),I=1,J)
   61 FORMAT (50X,9HALL ROOTS//2(28X,2HEV,28X,2HDN)//(4D30.16))
      WRITE (6,62) (EV(I),DEV(I),I=1,NEV)
   62 FORMAT (30X,37HEIGENVALUES HAVING DN LESS THAN DTEST//
     12(28X,2HEV,28X,2HDN)//(4D30.16))
      DO 20 L=1,NEV
   20 WRITE (6,63) (EV(L),DEV(L),N,VO,VOP)
   63 FORMAT(1H$,D23.16,D12.3,2X,2HN=I2,2X,3HVO=F4.1,10X,4HVOP=F6.3)
      RETURN
      END
```

```
$IBFTC ZERO    LIST,REF,DECK
      SUBROUTINE ZERO
      DOUBLE PRECISION XSTART,STEP,XMAX,PRECSN,DTEST,XBEGIN,ROOT,DN
      DOUBLE PRECISION X,X1,X2,T1,T2,DABS,E,XTEST
      DOUBLE PRECISION W,H,A,VO,VOP
      INTEGER DWRITE
      COMMON COM
      EQUIVALENCE (A,COM(1)),(W,COM(3)),(H,COM(5)),(VO,COM(7)),
     1(N,COM(16)),(VOP,COM(325)),(ROOT,COM(9)),(XSTART,ESTART,COM(11)),
     2(STEP,COM(797)),(PRECSN,COM(799)),(XMAX,EMAX,COM(801)),
     3(XTEST,COM(811)),(DTEST,COM(803)),(DN,COM(805)),
     4(E,X,COM(327)),(DWRITE,COM(796)),(XBEGIN,COM(809))
      X = XBEGIN
      CALL CALC
      GO TO (101,102),DWRITE
  101 WRITE (6,61) E,DN
   61 FORMAT(10X,2(D28.16))
  102 IF (DN) 1,2,3
    1 J = 1
      GO TO 4
    2 ROOT = X
      IF(DWRITE.EQ.2) GO TO 15
  120 WRITE (6,63) ROOT,DN
   63 FORMAT(10X,2(D28.16),4HROOT)
  121 GO TO 15
    3 J = 2
    4 X1 = X
      T1 = DN
      X = X1+STEP
      CALL CALC
      IF(DWRITE.EQ.2) GO TO 104
  103 WRITE(6,61) E,DN
  104 IF (DN) 5,2,6
    5 GO TO (7,8),J
    6 GO TO (8,7),J
    7 IF (X-XMAX) 4,14,14
    8 T2 = DN
      X2 =X
    9 X = (DABS(T1)*X2 + DABS(T2)*X1)/(DABS(T1)+DABS(T2))
      IF(X2-X.LE.PRECSN) GO TO 16
   10 CALL CALC
      IF(DWRITE.EQ.2) GO TO 106
      WRITE(6,61) E,DN
  106 IF (DN) 11,2,12
   11 GO TO (13,8),J
   12 GO TO (8,13),J
   13 X1 = X
      T1 = DN
      X = (DABS(T1)*X2 + DABS(T2)*X1)/(DABS(T1)+DABS(T2))
      IF (X-X1 -PRECSN) 17,17,10
   16 J2=2
      GO TO 18
   17 J2=1
   18 CALL CALC
      IF(DABS(DN).GT.DTEST) GO TO 20
   19 J1=1
      GO TO 21
   20 J1=2
   21 GO TO (2,22),J1
   22 GO TO (23,24),J2
   23 IF (X-X1-XTEST )25,25,10
   24 IF(X2-X-XTEST)25,25,10
   25 ROOT = X
      GO TO (107,108),DWRITE
  107 WRITE (6,62) E,DN
   62 FORMAT (10X,2(D28.16),12HDN TOO LARGE)
  108 CALL SLITE (3)
      GO TO 15
   14 CALL SLITE (1)
   15 RETURN
      END
```

```
      SUBROUTINE CALC
      INTEGER EVCLC
      SUBROUTINE CALC
      INTEGER EVCLC
      DOUBLE PRECISION W,H,A,VO,VOP
      DOUBLE PRECISION DN,E,DABS,DSQRT,GOW,WGOW,RGOW,RBGOW,XI,XJ,XN
      DOUBLE PRECISIONBGJH,BGIW,ABGJH,ABGIW,GJH,GIW,RGIW,RGJH,RBGJH
      DOUBLE PRECISION EXPP   , DEXP   , THGJH  , EXPN   , CSHF
      DOUBLE PRECISION SNHF   , CSF    , DCOS   , SNF    , DSIN
      DOUBLE PRECISION RBGIW,XN,BGNH,ABGNH,GNH,ETA,CS,TWGIW,THGNH
      COMMON COM
      EQUIVALENCE (A,COM(1)),(W,COM(3)),(H,COM(5)),(VO,COM(7)),
     1(N,COM(16)),(VOP,COM(325)),(ROOT,COM(9)),(XSTART,ESTART,COM(11)),
     2(E,X,COM(327)),(EVODD,COM(329)),(DN,COM(805))
      EQUIVALENCE (RGOW,RGIW),(RBGOW,RBGIW)
C SUBROUTINE SYMBOLS RGIW,RBGIW,RGJH,RBGJH CORRESPOND TO TEXT
C  SYMBOLS SNW,SNW-BAR,SNH,SNH-BAR,RESPECTIVELY
  701 ETA =0.512335100
  702 GOW = ETA*DSQRT(E)
  703 WGOW=W*GOW
      GO TO (704,705),EVODD
  704 RGOW =-DCOS(WGOW)
      RBGOW =GOW*DSIN(WGOW)
      GO TO 200
  705 RBGOW = -DCOS(WGOW)
      IF (WGOW .EQ. 0.D0) GO TO 706
      RGOW = -DSIN(WGOW)/GOW
      GO TO 200
  706 RGOW = -W
  200 DO 300 I=1,N
      J=I-1
      XI=I
      XJ =J
      BGJH= E- XJ**2*VOP-VO
      BGIW = E- XI**2*VOP
      ABGIW=DABS(BGIW)
      ABGJH=DABS(BGJH)
      GJH = ETA*DSQRT(ABGJH)
      GIW = ETA*DSQRT(ABGIW)
      TWGIW = 2.D0 * W*GIW
      THGJH = 2.D0 *H* GJH
      IF(BGJH) 1,2,3
    1 EXPP= DEXP(THGJH)
      EXPN = DEXP(-THGJH)
      CSHF = (EXPP+ EXPN)/2.D0
      SNHF = (EXPP- EXPN)/2.D0
      RGJH  = - (RGIW*CSHF + RBGIW*SNHF/GJH)
      RBGJH  = -(RGIW*GJH*SNHF +RBGIW*CSHF)
      GO TO 210
    2 RGJH =-(RGIW+2.D0*H*RBGIW)
      RBGJH =-RBGIW
      GO TO 210
    3 CSF = DCOS(THGJH)
      SNF = DSIN(THGJH)
      RGJH  = -(RGIW*CSF + RBGIW*SNF/GJH)
      RBGJH  = RGIW*GJH*SNF - RBGIW*CSF
  210 IF(BGIW) 201,202,203
  201 EXPP= DEXP(TWGIW)
      EXPN = DEXP(-TWGIW)
      CSHF = (EXPP+ EXPN)/2.D0
      SNHF = (EXPP- EXPN)/2.D0
      RGIW  = -(RGJH*CSHF + RBGJH*SNHF/GIW)
      RBGIW  = -(RGJH*GIW*SNHF +RBGJH*CSHF)
      GO TO 300
  202 RGIW =-(RGJH+2.D0*W*RBGJH)
      RBGIW =-RBGJH
      GO TO 300
  203 CSF = DCOS(TWGIW)
      SNF = DSIN(TWGIW)
      RGIW  = -(RGJH*CSF + RBGJH*SNF/GIW)
      RBGIW  = RGJH *GIW*SNF -RBGJH*CSF
  300 CONTINUE
      XN =N
      BGNH = E-XN**2*VOP-VO
      ABGNH= DABS(BGNH)
      GNH = ETA*DSQRT(ABGNH)
      THGNH = 2.D0*H*GNH
      IF(BGNH) 301,302,303
  301 EXPP= DEXP(THGNH)
      EXPN = DEXP(-THGNH)
      CSHF = (EXPP+ EXPN)/2.D0
      SNHF = (EXPP- EXPN)/2.D0
  311 DN = -(RGIW*CSHF+ RBGIW*SNHF/GNH)
      GO TO 600
  302 DN=-(RGIW+2.D0*H*RBGIW)
      GO TO 600
  303 CSF = DCOS(THGNH)
      SNF = DSIN(THGNH)
  313 DN = -(RGIW*CSF * RBGIW*SNF/GNH)
  600 RETURN
      END
```

APPENDIX E

FORTRAN IV PROGRAM FOR COMPUTATIONS OF WAVE FUNCTIONS

General Description

Like the eigenvalue program, this program operates with the Lewis 7094 monitor system. It consists of the same MAIN listed in appendix D plus eight subroutines. The following is a description of the primary functions of the routines:

MAIN determines what is to be computed (eigenvalues or wave functions) and stores the values of the parameters to be used by the subroutines in computing the wave functions.

Subroutine VOPFIX fixes the value of $V_M(x')$ to be used in the computations and feeds eigenvalues to subroutine NORMAL.

Subroutine NORMAL computes and stores ratios of coefficients of sin- and cos-like terms in each interval (the A_n's and B_n's in eqs. (45) to (47)) to the arbitrary coefficient in the 0^{th} well. (These quantities are the α_n's and β_n's of eqs. (C15) to (C18).) It also normalizes the wave function by finding the value of the B_0^w (or A_0^w) that will make

$$\int_{-\infty}^{\infty} |\lambda(x')|^2 \, dx' = 1$$

in accordance with the procedure in appendix C.

Subroutine WFC computes the normalized A_n's and B_n's and sends them to other subroutines to be used in computing actual values of the wave function in the entire range $x' = 0$ to $(N + 1)a - w$. The other subroutines return the wave function values to WFC, which prints them all out and determines whether or not a plot should also be made.

Subroutine WFO computes values of $\lambda_0^w(x')$, $\lambda_0^h(x')$, $|\lambda_0^w(x')|^2$, and $|\lambda_0^h(x')|^2$ and returns these values to WFC.

Subroutine WFXIW computes values of $\lambda_n^w(x')$ and $|\lambda_n^w(x')|^2$ for $n > 0$ and returns these values to WFC.

Subroutine WFXIH computes values of $|\lambda_n^h(x')|$ and $|\lambda_n^h(x')|^2$ for $n > 0$ (including $n = N$) and returns these values to WFC.

Subroutine PLOTFX sets up PLOTMY.

Subroutine PLOTMY furnishes a plot of $\lambda(x')$ and $|\lambda(x')|^2$ against x'. (This subroutine is part of the library tape of the Lewis Monitor System.)

Details of Individual Routines

In the following descriptions only those parts of MAIN and VOPFIX pertaining to computations of the wave functions are included.

In MAIN the parameters N, w, h, a, and V_0 as well as the choice of how $V_M(x')$ is to be made are fed in as described in appendix D. EVSKIP must be set equal to 1 so that eigenvalues will not be computed. In addition, JEV must be fixed, which gives the total number of eigenvalue data cards to be used in the run.

Next, the number of subintervals in each region of constant potential is fixed. Provision is made for computing wave functions only in certain regions if desired. Then a decision is made as to whether a plot is to be obtained in addition to the printed values for $\lambda(x')$. If a plot is asked for, various parameters needed by PLOTMY are then read in. Control is then transferred to the same DO-loop that sets V_0 as described in appendix D at the end of which the program is terminated.

Subroutine VOPFIX will determine the value of $V_M(x')$ to be used in subsequent subroutines as described in appendix D. However, if EVSKIP was set equal to 1 in MAIN, then instead of calling EVFIND, control will be transferred to an interval DO-loop that will read eigenvalues stored in MAIN one at a time and call NORMAL. When this procedure has been followed JEV times (see MAIN), the value of $V_M(x')$ in the external DO-loop is stepped up and the inner DO-loop cycle repeated. When the outer DO-loop is completed, control is returned to MAIN.

It should be noted that a dummy subroutine EVFIND must be included in the deck when computing wave functions or the program will not run.

Subroutine NORMAL computes A_n^w/B_0^w, B_n^w/B_0^w, A_n^h/B_0^w, and B_n^h/B_0^w (see eqs. (C13) to (C18)) from the matching equations (A4), (A5), (A7), (A8), (A9), (A10), and (A11). As explained in the text, if DN is small enough for the eigenvalue being used, the results will be the same as if equation (A12) had been used instead of equation (A11). The routine is set up in such a manner that individual quantities needed for the normalization as given by equations (C21), (C22), (C23), (C24), and (C9) are computed and stored along with each ratio. After all of the ratios have been computed and stored and the normalization of the arbitrary coefficient has been completed, WFC is called.

Subroutine WFC normalizes and stores the unnormalized coefficients computed in NORMAL. Then A_0^h, B_0^h, and G_0^h are computed and WFO is called. Next, a DO-loop is entered in which the following procedure is carried out:

First, a test is made to determine whether $\lambda(x')$ was desired for the region being considered. If the data in MAIN indicated that no $\lambda(x')$ was asked for the region in question, then the same test is made for the next region one atomic distance farther along the positive half of the chain. If the test indicates that $\lambda(x')$ was asked for in the region, then A_n^w, B_n^w, and B_n^w are set up and WFXIW is called to compute $\lambda(x')$ in the well portion of the region.

When WFXIW returns control to WFC, A_n^h, B_n^h, and G_n^h are set up and WFXIH is called to compute $\lambda(x')$ in the hill protion of the region. Following this, the test is applied to the next region.

After all of the regions in the chain have been tested and values of $\lambda(x')$ computed for all of the region for which these values are requested, the values are printed out.

Then if a plot is desired (KPLOT = 1), PLOTFX is called. If no plot is desired, control is returned to NORMAL.

The special subroutine WFO was written to compute $\lambda_0^w(x')$ and $\lambda_0^h(x')$ because the beginning and end of the cycle have somewhat special behavior. These quantities and their absolute squares are computed by using equations (24) and (25). Control is then returned to WFC.

Subroutine WFXIW computes the quantities $\lambda_n^w(x')$ and $|\lambda_n^w(x')|^2$ (for $0 < n \leq N$) using equation (38). Control is returned to WFC.

Subroutine WFXIH computes the quantities $\lambda_n^h(x')$ and $|\lambda_n^h(x')|^2$ for $0 < n < N$ by using equation (39). When a test indicates that $n = N$, then $\lambda_N^h(x')$ and $|\lambda_N^h(x')|$ are computed by using equation (40). After each set of computations control is returned to WFC.

Subroutine PLOTFX(EV) arranges the values of x', $\lambda_n(x')$, and $|\lambda_n(x')|^2$ in arrays so that they can be plotted properly by PLOTMY. All of the input control data for this subroutine is read in by MAIN. The eigenvalue is an argument of this subroutine and is read in by VOPFIX. Actually, the eigenvalue is only required for the legend of the plot.

Subroutine PLOTMY is part of the library tape of the Lewis monitoring system. It is the routine that actually plots $\lambda(x')$ and $|\lambda(x')|^2$ against x'. The main feature of this routine that must be taken into account is that it places the ordinate across the top of the page with zero to the left and the abscissa down the page with the lowest value at the top. While this feature is somewhat inconvenient in many cases, it has the advantage of permitting the case of an abscissa of arbitrary length since several pages can be covered continuously. Its use is fully described in reference 16.

Input Data

Units for the input data are the following: energy, electron volts; length, angstroms.

The data are input from tape 5. The names of the quantities for which the data are used along with a description of the quantity are now listed. The subroutines in which these quantities are used follow each description.

N number of atoms in positive half of chain (MAIN, VOPFIX, NORMAL, WFC, WFXIH, PLOTFX)

W width of well portion in one period of $V_P(x')$ (MAIN, NORMAL, WFO, WFXIW)

H width of hill portion in one period of $V_P(x')$ (MAIN, NORMAL, WFO, WFXIH)

A distance of atomic separation (MAIN, VOPFIX, NORMAL, WFXIW, WFXIH)

KI see appendix D

KF see appendix D

KS see appendix D

VPSLCT see appendix D

VPCHS see appendix D

KIP see appendix D

KFP see appendix D

KSP see appendix D

IVSKIP see appendix D

EVODD see appendix D

NI beginning multiple of fraction of subdivision of individual region used for computing wave functions

NF 1/NF, fraction of subdivision of individual region; NF, final multiple of this subdivision

NS stepping interval of multiple of subdivision

JDO dimensional quantity by means of which the decision to compute $\lambda(x')$ for a region is made; each region in sequence is characterized by the location of the number on the data card - the first number on the card corresponds to the 0^{th} region; if the j^{th} column on the data card is blank, no computation of $\lambda_j(x')$ will be made; if the j^{th} column contains a 1, the computation is made (MAIN, WFC)

KPLOT 1, plot of $\lambda(x')$ will be made; 2, no plot of $\lambda(x')$ will be made

XDSIZE number of points on one curve in plot

LTM number of line spaces between grid lines on plot

LTN number of print spaces between grid lines on plot

KN number of curves on plot

KSX scaling parameter for x-scale (runs up and down the page); FX and DX will be multiplied by 10^{KSX-6}

FX quanti'‐ used to specify starting value on vertical scale; actual starting value, FX times 10^{KSX-6}

DX quantity used to specify change in value in vertical scale one line space; actual change, DX times 10^{KSX-6}

KSY scaling parameter for y-scale (runs across page); FY and DY will be multiplied by 10^{KSY-6}

FY quantity used to specify starting value on horizontal scale; actual starting value, FY times 10^{KSY-6}

DY quantity used to specify change in horizontal scale in one print space; actual change, DY times e^{KSY-6}

A listing of the subroutines used in computing the wave function follows (MAIN and VOPFIX are listed in appendix D).

```
      SUBROUTINE NORMAL(EV)
C FULL DOUBLE PRECSN. ONLY STORES FOR 50 ATOMS NOW.
      DIMENSION AKW(50),BKW(50),AKH(50),BKH(50),
     1GKW(50),GKH(50),JW(50),JH(50),RMLZ(105)
      DOUBLE PRECISION W,H,VO,VOP,BOW,GIW,GJH,AKW,BKW,AKH,BKH,GKW,GKH
      DOUBLE PRECISION DABS,DSQRT,EV,EX,BGJH,ABGJH,BGIW,ABGIW,XI,RML
      DOUBLE PRECISION  SNF    , DSIN   , TWGIW  , EXPP   , DEXP
      DOUBLE PRECISION  FHGJH  , EXPN   , SNHF   , CNHF   , CNF
      DOUBLE PRECISION  DCOS   , WGIW   , EXPPJH , THGJH  , EXPNJH
      DOUBLE PRECISION  SNHFJH , CNHFJH , EXPPIW , FWGIW  , EXPNIW
      DOUBLE PRECISION  SNHFIW , CNHFIW , SNFJH  , CNFJH  , SNFIW
      DOUBLE PRECISION  CNFIW,RMLZ,ETA
      DOUBLE PRECISION AANMOH,BBNMOH,ABNMOH,AANMIW,BBNMIW,ABNMIW
      DOUBLE PRECISION AANMJH,BBNMJH,ABNMJH
      INTEGER EVODD
      COMMON  COM
      EQUIVALENCE (A,COM(1)),(W,COM(3)),(H,COM(5)),(VO,COM(7)),
     1(VOP,COM(325)),(BOW,COM(9503)),(AKW,COM(9505)),(BKW,COM(9605)),
     2(AKH,COM(9705)),(BKH,COM(9805)),(GKW,COM(9905)),(GKH,COM(10005)),
     3(N,COM(16)),(JH,COM(10105)),(JW,COM(10205)),(EVODD,COM(329))
    1 EX = EV
      ETA = 0.51233510O
      AKW(1) = 0.0D0
      BKW(1) = 0.0D0
      GIW = ETA*DSQRT(EX)
      GKW(1) = GIW
      WGIW = W*GIW
      TWGIW = 2.D0*WGIW
      BGJH = EX-VO
      ABGJH = DABS(BGJH)
      GJH = ETA*DSQRT(ABGJH)
      GKH(1) = GJH
      THGJH = 2.D0*H*GJH
      FHGJH = 4.D0*H*GJH
      JW(1) = 3
CCOMPUTE COEFFICIENT OF BOW OR AOW IN RMLZ
      SNF = DSIN(TWGIW)
C TERM IN NORMALIZATION INVOLVING BOW OR AOW
      GO TO (101,102),EVODD
  101 RMLZ(1) = W*(1.D0+SNF/TWGIW)/2.D0
C COMPUTE BOH/BOW
      BKH(1) = DCOS(WGIW)
      GO TO 103
  102 RMLZ (1) = W*(1.D0 -SNF/TWGIW)/(2.D0*GIW**2)
C COMPUTE BOH/AOW
      BKH(1) = DSIN(WGIW)/GIW
C COMPUTE COEFFS OF AOH**2,BOH**2,AND AOH*BOH IN RMLZ
  103 IF (BGJH) 2,3,4
    2 JH(1) = 1
      EXPP = DEXP(FHGJH)
      EXPN = DEXP(-FHGJH)
      SNHF = (EXPP-EXPN)/2.D0
      CNHF = (EXPP+EXPN)/2.D0
C (1/H)* COEFF OF (AOH)**2 IN RMLZ
      AANMOH = SNHF/FHGJH-1.D0
C (1/H)* COEFF OF BOH**2 IN RMLZ
      BBNMOH = SNHF/FHGJH+1.D0
C (1/2H)* COEFF OF AOH*BOH IN RMLZ
      ABNMOH = (CNHF-1.D0)/FHGJH
      GO TO 5
```

```
    3 JH(1) = 2
      AANMOH = 2.D0*(2.D0*H)**2/3.D0
      BBNMOH = 2.D0
      ABNMOH = 2.D0*H
      GO TO 5
    4 JH(1) = 3
      SNF = DSIN(FHGJH)
      CNF = DCOS(FHGJH)
      AANMOH = 1.D0-SNF/FHGJH
      BBNMOH = 1.D0+SNF/FHGJH
      ABNMOH = (1.D0-CNF)/FHGJH
    5 GO TO (106,107),EVODD
C COMPUTE AOH/BOW
  106 SNF = DSIN(WGIW)
      AKH(1) = -GIW*SNF
      GO TO 108
C COMPUTE AOH/AOW
  107 AKH(1) = DCOS(WGIW)
  108 JHK = JH(1)
      GO TO (6,7,6),JHK
    6 AKH(1) = AKH(1)/GJH
C TERM IN RMLZ DUE TO ZERUTH HILL
    7 RMLZ(2) = H*(AANMOH*AKH(1)**2+BBNMOH*BKH(1)**2
     1+2.D0*ABNMOH*AKH(1)*BKH(1))
      DO 40  I=1,N
      XI = I
      I1 = I+1
      BGIW = EX-XI**2*VOP
      ABGIW = DABS(BGIW)
      GIW = ETA*DSQRT(ABGIW)
      GKW(I1) =GIW
      TWGIW = 2.D0*W*GIW
      FWGIW = 4.D0*W*GIW
      GO TO(8,9,10),JHK
C COMPUTE BIW/BOW
    8 EXPPJH = DEXP(THGJH)
      EXPNJH = DEXP(-THGJH)
      SNHFJH = (EXPPJH-EXPNJH)/2.D0
      CNHFJH = (EXPPJH+EXPNJH)/2.D0
      BKW(I1) = AKH(I)*SNHFJH+BKH(I)*CNHFJH
      AKW(I1) = GKH(I)*(AKH(I)*CNHFJH+BKH(I)*SNHFJH)
      GO TO 11
    9 BKW(I1) = 2.D0*H*AKH(I)+BKH(I)
      AKW (I1) = AKH(I)
      GO TO 11
   10 SNFJH = DSIN(THGJH)
      CNFJH = DCOS(THGJH)
      BKW(I1) = AKH(I)*SNFJH+BKH(I)*CNFJH
      AKW(I1) = GKH(I)*(AKH(I)*CNFJH-BKH(I)*SNFJH)
   11 IF (BGIW) 12,13,14
   12 JW(I1) = 1
C COMPUTE COEFFS OF AIW**2,BIW**2,AIW*BIW IN RMLZ
      EXPPIW = DEXP(FWGIW)
      EXPNIW = DEXP(-FWGIW)
      SNHFIW = (EXPPIW-EXPNIW)/2.D0
      CNHFIW = (EXPPIW+EXPNIW)/2.D0
C (1/W)*COEFF OF AIW**2
      AANMIW = SNHFIW/FWGIW-1.D0
C (1/W)*COEFF OF BIW**2
      BBNBIW = SNHFIW/FWGIW+1.D0
C (1/2W)*COEFF OF AIW*BIW
      ABNMIW = (CNHFIW-1.D0)/FWGIW
      GO TO 15
```

```
   13 JW(I1) = 2
      AANMIW = 2.D0*(2.D0*W)**2/3.D0
      BBNMIW = 2.D0
      ABNMIW = 2.D0*W
      GO TO 15
   14 JW(I1) = 3
      SNFIW = DSIN(FWGIW)
      CNFIW = DCOS(FWGIW)
      AANMIW = 1.D0-SNFIW/FWGIW
      BBNMIW = 1.D0+SNFIW/FWGIW
      ABNMIW = (1.D0-CNFIW)/FWGIW
   15 JWK = JW(I1)
C COMPUTE AIW/BOW
      GO TO (20,21,20),JWK
   20 AKW(I1) = AKW(I1)/GIW
C TERM IN RMLZ DUE TO ITH WELL
   21 I2 = 2*I+1
      RMLZ(I2) = W*(AANMIW*AKW(I1)**2+BBNMIW*BKW(I1)**2
     1+2.D0*ABNMIW*AKW(I1)*BKW(I1))
C COMPUTE QUANTITIES FOR ITH HILL
   22 BGJH = BGIW-VO
      ABGJH = DABS(BGJH)
      GJH = ETA*DSQRT(ABGJH)
      GKH(I1) = GJH
      THGJH = 2.D0*H*GJH
      FHGJH = 4.D0*H*GJH
C COMPUTE COEFF OF AJH**2,BJH**2, AND AJH*BJH IN RMLZ
      IF (BGJH) 23,24,25
   23 JH(I1) = 1
C EXPPJH AND EXPNJH NOT SAME AS THOSE USED BETWEEN 8 AND 9
      EXPPJH = DEXP(FHGJH)
      EXPNJH = DEXP(-FHGJH)
      SNHFJH = (EXPPJH-EXPNJH)/2.D0
      CNHFJH = (EXPPJH+EXPNJH)/2.D0
C (1/H)*COEFF OF AJH **2
   28 AANMJH = SNHFJH/FHGJH-1.D0
C (1/H)*COEFF OF BJH **2
      BBNMJH = SNHFJH/FHGJH+1.D0
      ABNMJH = (CNHFJH-1.D0)/FHGJH
      GO TO 33
   24 JH(I1) =2
   30 AANMJH = 2.D0*(2.D0*H)**2/3.D0
      BBNMJH = 2.D0
      ABNMJH = 2.D0*H
      GO TO 33
   25 JH(I1) =3
      SNFJH = DSIN(FHGJH)
      CNFJH = DCOS(FHGJH)
   32 AANMJH = 1.D0-SNFJH/FHGJH
      BBNMJH = 1.D0+SNFJH/FHGJH
      ABNMJH =.(1.D0-CNFJH)/FHGJH
   33 JHK = JH(I1)
      GO TO (27,29,31),JWK
```

```
C EXPPIW AND EXPNIW DIFFERENT FROM THOSE BETWEEN 12 AND 13
   27 EXPPIW = DEXP(TWGIW)
      EXPNIW = DEXP(-TWGIW)
      SNHFIW = (EXPPIW-EXPNIW)/2.D0
      CNHFIW = (EXPPIW+EXPNIW)/2.D0
      IF (I-N.GE.0) GO TO 41
C COMPUTE BJH/BOW
      BKH(I1) = AKW(I1)*SNHFIW + BKW(I1)*CNHFIW
C COMPUTE AJH/BOW
      AKH(I1) = GIW*(AKW(I1)*CNHFIW+BKW(I1)*SNHFIW)
      GO TO 26
      BKH(I1) = 2.D0*W*AKW(I1)+BKW(I1)
   29 IF (I-N.GE.0) GO TO 41
      AKH(I1) = AKW(I1)
      GO TO 26
   31 SNFIW = DSIN(TWGIW)
      CNFIW = DCOS(TWGIW)
      IF (I-N.GE.0) GO TO 41
      BKH(I1) = AKW(I1)*SNFIW+BKW(I1)*CNFIW
      AKH(I1) = GIW*(AKW(I1)*CNFIW-BKW(I1)*SNFIW)
   26 GO TO (38,39,38),JHK
   38 AKH(I1) = AKH(I1)/GJH
C TERM IN RMLZ DUE TO ITH HILL
   39 I3 = I2+1
      RMLZ(I3) = H*(AANMJH*AKH(I1)**2+BBNMJH*BKH(I1)**2
     1+2.D0*ABNMJH*AKH(I1)*BKH(I1))
   40 CONTINUE
C COMPUTE QUANTITES FOR LAST HILL
   41 N1 = N+1
      BKH(N1) = 0.D0
      GO TO (42,43,44),JWK
   42 AKH(N1) = AKW(N1)*SNHFIW+BKW(N1)*CNHFIW
      GO TO 45
   43 AKH(N1) = 2.D0*W*AKW(N1)+BKW(N1)
      GO TO 45
   44 AKH(N1) = AKW(N1)*SNFIW+BKW(N1)*CNFIW
   45 IF (BGJH) 46,47,48
   46 EXPPJH = DEXP(THGJH)
      EXPNJH = DEXP(-THGJH)
      SNHFJH = (EXPPJH-EXPNJH)/2.D0
      AKH(N1) = -AKH(N1)/SNHFJH
C (1/H)*COEFF OF AKH(N+1)**2 IN RMLZ
      EXPPJH = DEXP(FHGJH)
      EXPNJH = DEXP(-FHGJH)
      SNHFJH = (EXPPJH-EXPNJH)/2.D0
      AANMJH = SNHFJH/FHGJH-1.D0
      GO TO 49
   47 AKH(N1) = -AKH(N1)/(2.D0*H)
      AANMJH = 2.D0*(2.D0*H)**2/3.D0
      GO TO 49
   48 SNFJH = DSIN(THGJH)
      AKH(N1) = -AKH(N1)/SNFJH
      SNFJH = DSIN(FHGJH)
      AANMJH = 1.D0-SNFJH/FHGJH
C LAST ENTRY IN RMLZ
   49 N2 =2*N1
      RMLZ(N2) = H*AANMJH*AKH(N1)**2
      RML = 0.D0
      DO 50  J=1,N2
   50 RML = RML + RMLZ(J)
   51 BOW = DSQRT(1.D0/(2.D0*RML))
      CALL WFC(EV)
      RETURN
      END
```

```
      SUBROUTINE WFC(EV)
      DOUBLE PRECISICN AKW,BKW,AKH,BKH,GKW,GKH,EV,VO,VOP
      DIMENSION JDO(100),AKW(50),BKW(50),AKH(50),BKH(50),
     1GKW(50),GKH(50),XP(220),WF(220),WFSQ(220)
      INTEGER EVCDD
      COMMON  COM
      EQUIVALENCE (A,COM(1)),(W,COM(3)),(H,COM(5)),(VO,COM(7)),
     1(N,COM(16)),(VCP,COM(325)),(ROOT,COM(9)),(XSTART,ESTART,COM(11)),
     T(NI,COM(17)),(NF,COM(18)),(NS,COM(19)),(JDO,COM(225)),
     2(KPLOT,COM(574)),(IK1,COM(575)),(XP,COM(576)),(WF,COM(896)),
     3(WFSQ,COM(1116)),(BOW,COM(9503)),(AKW,COM(9505)),(BKW,COM(9605)),
     4(AKH,CCM(9705)),(BKH,CCM(9805)),(GKW,COM(9905)),(GKH,COM(10005)),
     5(EVODD,CCM(329))
      GO TO (1,1C1),EVODD
    1 BKW(1) = BCW
      GO TO 102
  101 AKW(1) = BCW
  102 N1 = N+1
      DO 2 J=1,N
      J1= J+1
      AKW(J1) = BOW*AKW(J1)
      BKW(J1) = BOW*BKW(J1)
      AKH(J) = BOW*AKH(J)
    2 BKH(J) = BOW* BKH(J)
      AKH(N1) = BOW*AKH(N1)
      BKH(N1) = 0.0D0
C ALL COEFFS NOW NORMALIZED AND STORED
      IK1 = 0
      IF (JDC(1)) 4,4,3
    3 IK1=IK1 +1
      ANH = AKH(1)
      BNH = BKH(1)
      GOW = GKW(1)
      GOH = GKH(1)
      CALL WFO(ANH,BNH,GOW,GOH)
    4 JD = NF/NS
      DO 10 I=2,N1
      IF (JDC(I)) 10,10,5
    5 IF (I-N1) 7,6,6
    6 CALL SLITE (2)
    7 IK1 = IK1 +1
      ANW = AKW(I)
      BNW = BKW(I)
      GIW = GKW(I)
      CALL WFXIW(ANW,BNW,GIW,I)
      IF (I-N1) 8,11,11
    8 ANH = AKH(I)
      BNH = BKH(I)
      GJH = GKH(I)
      CALL WFXIH(ANH,BNH,GJH,I)
   1C CONTINUE
   11 CALL SLITET(2,KOOOFX)
       GC TO(12,13),KOOOFX
   12 ANH = AKH(N1)
      BNH = 0.0
      GJH = GKH(N1)
      CALL SLITE (2)
      CALL WFXIH(ANH,BNH,GJH,I)
   13 WRITE (6,61) VC,VOP,EV,BOW,EVODD
   61 FORMAT (1HK,10X,3HVO=F5.1,5X,4HVOP=F15.9,5X,3HEV=1PD23.15,5X,
     14HBOW=1PE15.7,5X,6HEVOCD=I2///
     22(4X,3HXPW,6X,4HWFIW,4X,6HWFIWSQ,4X,3HXPH,7X,4HWFIH,4X,6HWFIHSQ))
      NPLOT = N/2 +1
      DO 14 IA= 1,NPLOT
      K= 40*(IA-1) +1
      L=K+9
      WRITE (6,63)
   63 FORMAT (1HK)
      WRITE (6,62)((XP(J),WF(J),WFSQ(J),XP(J+10),WF(J+10),    WFSQ(J+10),
     1XP(J+20),WF(J+20),WFSQ(J+20),XP(J+30),WF(J+30),         WFSQ(J+30))
     2,J=K,L)
   62 FORMAT (4(CPF8.3,1PE10.2,1PE10.2))
   14 CONTINUE
      GO TO (15,16),KPLOT
   15 CALL PLOTFX(EV)
   16 RETURN
      END
```

```
      SUBROUTINE WFO(AHN,BHN,GOW,GOH)
      DIMENSION XP(220),WF(220), WFSQ(220),JH(100)
      INTEGER EVODD
      COMMON  COM
      EQUIVALENCE (W,COM(3)),(H,COM(5)),(NI,COM(17)),(NF,COM(18)),
     1(NS,COM(19)),(XP,COM(576)),(WF,COM(896)),(WFSQ,COM(1116)),
     2(BOW,COM(9503)),(JH,COM(10105)),(EVODD,COM(329))
    1 JHK= JH(1)
      XNF = NF
      DO 10 K=NI,NF,NS
      XK = K
      XW = XK*W/XNF
      GXW = GOW*XW
      XP(K) = XW
      GO TO (11,12), EVODD
   11 WF(K) = BOW* COS(GXW)
      GO TO 13
   12 WF(K) = BOW*SIN(GXW)/GOW
   13 WFSQ(K) = WF(K) **2
      XH = 2.0*H*XK/XNF
      GXH = GOH*XH
      J= K+10
      XP(J) = XH + W
      GO TO (2,3,4), JHK
    2 WF(J) = AHN* SINH(GXH) + BHN* COSH(GXH)
      GO TO 5
    3 WF(J) = AHN* XH + BHN
      GO TO 5
    4 WF(J) = AHN* SIN(GXH) + BHN* COS(GXH)
    5 WFSQ(J) = WF(J)**2
   10 CONTINUE
      RETURN
      END
```

```
      SUBROUTINE WFXIW(ANW,BNW,GIW,I)
      DIMENSION XP(220),WF(220),WFSQ(220),JW(100)
      COMMON  COM
      EQUIVALENCE (A,COM(1)),(W,COM(3)),(N,COM(16)),
     1(NI,COM(17)),(NF,COM(18)),(NS,COM(19)),
     2(XP,COM(576)),(WF,COM(896)),(WFSQ,COM(1116)),(JW,COM(10205))
    1 I=I
      JWK = JW(I)
      XI = I-1
      XNF = NF
      DO 10 K= NI,NF,NS
      XK = K
      XW = 2.0*W*XK/XNF
      XPW = XI*A-W + XW
      GXPW = GIW*XW
      KP = 20*(I-1) + K
      XP(KP) = XPW
      GO TO (2,3,4),JWK
    2 WF(KP) = ANW*SINH(GXPW) + BNW* COSH(GXPW)
      GO TO 5
    3 WF(KP) = ANW*XW + BNW
      GO TO 5
    4 WF(KP) = ANW*SIN(GXPW) + BNW* COS(GXPW)
    5 WFSQ(KP) = WF(KP) **2
   10 CONTINUE
      RETURN
      END
```

```
      SUBROUTINE WFXIH(ANH,BNH,GJH,I)
      DIMENSION XP(220),WF(220),WFSQ(220),JH(100)
      COMMON  COM
      COMMON  COCOCM (10210)
      EQUIVALENCE (A,COM(1)),(W,COM(3)),(H,COM(5)),(N,COM(16)),
     1(NI,COM(17)),(NF,COM(18)),(NS,COM(19)),
     2(XP,COM(576)),(WF,COM(896)),(WFSQ,COM(1116)),(JH,COM(10105))
    1 I=I
      JHK = JH(I)
      XN = N
      XI = I-1
      XNF = NF
      CALL SLITET(2,K000FX)
       GO TO(11,6),K000FX
    6 DO 10 K= NI,NF,NS
      XK = K
      XH = 2.0*H*XK/XNF
      XPH = XI*A +W +XH
      GXPH = GJH*XH
      KP = 20*(I-1) + K +10
      XP(KP) = XPH
   20 GO TO (2,3,4),JHK
    2 WF(KP) = ANH*SINH(GXPH) + BNH* COSH(GXPH)
      GO TO 5
    3 WF(KP) = ANH*XH + BNH
      GO TO 5
    4 WF(KP) = ANH*SIN(GXPH) + BNH* COS(GXPH)
    5 WFSQ(KP) = WF(KP) **2
   10 CONTINUE
      GO TO 15
   11 DO 12 K = NI,NF,NS
      XK = K
      XH = 2.0*H*XK/XNF
      XPH= XN*A + W +XH
      GXPH = GJH*(XPH -A*(XN + 1.0) + W)
      KP = 20*(I-1) + K +10
      XP(KP) = XPH
      GO TO (7,8,9),JHK
    7 WF(KP) = ANH*SINH(GXPH)
      GO TO 13
    8 WF(KP) = ANH*XH
      GO TO 13
    9 WF(KP) = ANH* SIN(GXPH)
   13 WFSQ(KP) = WF(KP) **2
   12 CONTINUE
   15 RETURN
      END
```

```
      SUBROUTINE PLOTFX(EV)
C PLOTS XP VERTICALLY
      DIMENSION XP(220),WF(220),WFSQ(220)
      DIMENSION XDOWN(215),YACROS(430),KKK(14),P(11)
      COMMON COM
      EQUIVALENCE (N,COM(16)),(VO,COM(7)),(VOP,COM(325)),
     1(XP,COM(576)),(WF,COM(896)),(WFSQ,COM(1116)),(EVODD,COM(329)),
     2(XDSIZE,COM(807)),(LTM,COM(814)),(LTN,COM(815)),(KN,COM(816)),
     3(KSX,COM(817)),(KSY,COM(818)),(FX,COM(819)),(DX,COM(820)),
     4(FY,COM(821)),(DY,COM(822))
      INTEGER XDSIZE,EVODD
    1 DO 10 IO = 1,5
      J = 2*IO
      XDOWN (IO) = XP(J)
      YACROS(IO) = WF(J)
      ISQ = XDSIZE + IO
   10 YACROS(ISQ) = WFSQ(J)
C WF AND WFSQ FOR ZEROTH WELL NOW STORED IN YACROS
    2 NPL = 20*(N+1)
      DO 20 I1 = 11,NPL
      J1 = I1 -5
      XDOWN(J1) =XP(I1)
      YACROS(J1) = WF(I1)
      JSQ = XDSIZE + J1
   20 YACROS (JSQ) = WFSQ(I1)
C ALL WF AND WFSQ NOW STORED IN YACROS
C KN IS THE NUMBER OF CURVES
      KKK(1) = 54
      KKK(2) = KN
C NO OF POINTS IS = TO THE VALUE OF XDSIZE
      KKK(3) = XDSIZE
      P(1) = 1.0
C LTM SPECIFIES NUMBER  LINE SPACES BETWEEN GRID LINES
      P(3)= LTM
C LTN SPECIFIES NUMBER OF PRINT SPACES BETWEEN GRID LINES
      P(4) = LTN
      P(6) = KSX
C FX USED TO SPECIFY STARTING VALUE OF VERTICAL SCALE
      P(7) = FX
C DX USED TO SPECIFY  CHANGE IN VERTCAL GRID VALUES EACH LINE SPACE
      P(8) =DX
      P(9) = KSY
C FY USED TO SPECIFY STARTING VALUE OF  HORIZONTAL SCALE
      P(10) = FY
C DY USED TO SPECIFY  CHANGE IN HORIZONTAL GRID VALUES EACH PRINT SPACE
      P(11) = DY
C TITLE
      WRITE (6,61) N,EVODD
   61 FORMAT(2HPT,40X,36HWAVE FUNCTION (*) AND WFSQ(+) FOR N= I3,5X,
     16HEVODD=I2)
    3 CALL PLOTMY(XDOWN,YACROS,KKK,P)
C LEGEND
      WRITE (6,62) VO,VOP,EV
   62 FORMAT (2HPL,30X,3HVO=F5.1,5X,4HVOP=1PE15.8,5X,3HEV=1PD23.16,
     13HDN=)
      RETURN
      END
```

REFERENCES

1. Lifshitz, I. M., Azbel, M. Ia., and Kaganov, M. I.: The Theory of Galvanomagnetic Effects in Metals. Soviet Phys.-JETP, vol. 4, no. 1, Feb. 1957, pp. 41-54.

2. Lifshitz, I. M., and Peschanskii, V. G.: Galvanomagnetic Characteristics of Metals with Open Fermi Surfaces, I. Soviet Phys.-JETP, vol. 8, no. 5, May 1959, pp. 875-883.

3. Harrison, W. A., and Webb, M. B., eds.: The Fermi Surface. John Wiley & Sons, Inc., 1960.

4. Cohen, Morrel H., and Falicov, L. M.: Effect of Spin-Orbit Splitting on the Fermi Surfaces of the Hexagonal-Close-Packed Metals. Phys. Rev. Letters, vol. 5, no. 12, Dec. 1960, pp. 544-546.

5. Falicov, L. M., and Cohen, Morrel H.: Spin-Orbit in the Band Structure of Magnesium and Other Hexagonal-Close-Packed Metals. Phys. Rev., vol. 130, no. 1, Apr. 1963, pp. 92-97.

6. Stark, R. W., Eck, T. G., and Gordon, W. L.: Galvanomagnetic Investigation of the Fermi Surface of Magnesium. Phys. Rev., vol. 133, no. 2A, Jan. 1964, pp. A443-A451.

7. Blount, E. I.: Bloch Electrons in a Magnetic Field. Phys. Rev., vol. 126, no. 5, June 1962, pp. 1636-1653.

8. Cohen, Morrel H., and Falicov, L. M.: Magnetic Breakdown of Crystals. Phys. Rev. Letters, vol. 7, no. 6, Sept. 1961, pp. 231-233.

9. Reitz, J. R.: Magnetic Breakdown in Metals. Jour. Phys. Chem. Solids, vol. 25, no. 1, Jan. 1964, pp. 53-58.

10. Pippard, A. B.: Quantization of Coupled Orbits in Metals. Proc. Roy. Soc. (London), ser. A, vol. 270, no. 1340, Oct. 30, 1962, pp. 1-13.

11. Kittel, Charles: Quantum Theory of Solids. John Wiley & Sons, Inc., 1963, pp. 217-218.

12. Seitz, Frederick: The Modern Theory of Solids. McGraw-Hill Book Co., Inc., 1940, pp. 583-599.

13. Whittaker, E. T., and Watson, G. N.: A Course of Modern Analysis. Cambridge Univ. Press, 1950, p. 339.

14. Peierls, Rudolph Ernst: Quantum Theory of Solids. Clarendon Press (Oxford), 1955, pp. 150-152.

15. Dellner, Lois T., and Moore, Betty Jo: An Optimized Printer Plotting System Consisting of Complementary 7090 (Fortran) and 1401 (SPS) Subroutines. I - Instructions for Users. NASA TN D-2174, 1964.

"The aeronautical and space activities of the United States shall be conducted so as to contribute . . . to the expansion of human knowledge of phenomena in the atmosphere and space. The Administration shall provide for the widest practicable and appropriate dissemination of information concerning its activities and the results thereof."

—NATIONAL AERONAUTICS AND SPACE ACT OF 1958

NASA SCIENTIFIC AND TECHNICAL PUBLICATIONS

TECHNICAL REPORTS: Scientific and technical information considered important, complete, and a lasting contribution to existing knowledge.

TECHNICAL NOTES: Information less broad in scope but nevertheless of importance as a contribution to existing knowledge.

TECHNICAL MEMORANDUMS: Information receiving limited distribution because of preliminary data, security classification, or other reasons.

CONTRACTOR REPORTS: Technical information generated in connection with a NASA contract or grant and released under NASA auspices.

TECHNICAL TRANSLATIONS: Information published in a foreign language considered to merit NASA distribution in English.

TECHNICAL REPRINTS: Information derived from NASA activities and initially published in the form of journal articles.

SPECIAL PUBLICATIONS: Information derived from or of value to NASA activities but not necessarily reporting the results of individual NASA-programmed scientific efforts. Publications include conference proceedings, monographs, data compilations, handbooks, sourcebooks, and special bibliographies.

Details on the availability of these publications may be obtained from:

SCIENTIFIC AND TECHNICAL INFORMATION DIVISION

NATIONAL AERONAUTICS AND SPACE ADMINISTRATION

Washington, D.C. 20546